The Effects of Receiver Tracking Phase Error on the Performance of the Concatenated Reed-Solomon/Viterbi Channel Coding System

K. Y. Liu

N81-33365

2

ACKNOWLEDGEMENT

ABSTRACT

This document presents both analytical and experimental results of the effects of receiver tracking phase error, caused by weak signal conditions on either the uplink or the downlink or both, on the performance of the concatenated Reed-Solomon (RS)/Viterbi channel coding system. The test results were obtained under an emulated S-band uplink and X-band downlink, two-way space communication channel in the Telecommunication Development Laboratory (TDL) of JPL with data rates ranging from 4 kHz to 20 kHz. It is shown that, with ideal interleaving, the concatenated RS/Viterbi coding system is capable of yielding large coding gains at very low bit error probabilities ($\leq 10^{-6}$) over the Viterbi-decoded convolutional-only coding system. The results also show that performance equivalent to ideal interleaving in the concatenated RS/Viterbi coding system is obtained with an interleaving depth greater than or equal to 4. Because of the large coding gains the use of concatenated RS/Viterbi coding scheme in deep-space missions will make it possible to perform high-rate data transmission in conjunction with two-way ranging or doppler measurements when weak signal conditions exist (on both the uplink and the downlink during two-way communication). Similarly for one-way communication under weak downlink conditions, this concatenated coding scheme will also provide more data rate protection than the Viterbi-decoded convolutional-only coding system. Finally, analytic results on the effects of receiver tracking phase errors on the performance of the concatenated RS/Viterbi channel coding system with antenna array combining are presented.

TABLE OF CONTENTS

v

5

LIST OF FIGURES

LIST OF TABLES

SECTION I

INTRODUCTION

The concatenated coded system was proposed by Forney (Ref. 1) to achieve very low error probabilities. Toward this goal, Odenwalder (Ref. 2) proposed a concatenated coding system using the Viterbi-decoded convolutional codes as the inner code and the Reed-Solomon (RS) codes as the outer code (see Figure 1). In Ref. 3, Odenwalder, et al showed by simulation that a 255-symbol, 16-error correcting (E = 16), RS code with 8-bit per symbol (J = 8) concatenated with a constraint length (K) 7, rate (R) 1/2 or 1/3 Viterbi-decoded convolutional code, is a cost-effective coding system for achieving very low error probabilities. Rice (Refs. 4 to 6) proposed the use of the concatenated RS/Viterbi coding and image data compression for efficient deep-space communication. Both Voyager (at Uranus encounter, 1986) and Galileo will utilize this RS/Viterbi channel in combination with data compression (Refs. 8 and 9). Several near-earth and deep-space flight projects such as the International Solar Polar Mission (ISPM) have also considered using the concatenated RS/Viterbi coding scheme. In Ref. 4, Rice also discussed the potential advantage of the concatenated RS/Viterbi system over the Viterbi-decoded convolutional-only coding system when phase errors exist in the receiver. In Ref. 7, Odenwalder showed more simulation results of the concatenated RS/Viterbi coding system performance and the sensitivities of the factors such as phase errors, interleaving level, etc., which may affect the concatenated coding system performance. In Ref. 10, the results of an experimental study of the concatenated RS/Viterbi coding system performance in a two-way space communication channel with strong uplink and downlink is presented.

The purpose of this document is to present both analytical and experimental results of the effects of receiver tracking phase error on the performance of the concatenated RS/Viterbi channel coding system. The experimental results are obtained under an emulated two-way deep-space communication channel with S-band uplink and X-band downlink in the Telecommunication Development Laboratory (TDL) of JPL. TDL equipments are almost identical to the ground station receiving equipments of the Deep Space Network (DSN). It will be shown that the concatenated RS/Viterbi coding scheme is capable of yielding large coding gains over the Viterbi-decoded convolutional-only coding system when weak signal conditions exist on either the uplink or the downlink or both. Also shown is an evaluation of the impact of different choices of interleaving depth.

Recently antenna array combining techniques have been proposed to increase the signal-to-noise ratio for future space flight missions (Ref. 11). The last part of this document will present some analytical results on the effects of tracking phase errors in the re..ivers on the RS/Viterbi coding system performance under the conditions of array combining.

1-2

1-3

DATA SOURCE →

OUTER CODER
RS ENCODER

INNER CODER
CONVOLU-TIONAL ENCODER

SPACECRAFT

SPACE CHANNEL

INNER DECODER
VITERBI DECODER

OUTER DECODER
RS DECODER

GROUND STATION

→ DATA SINK
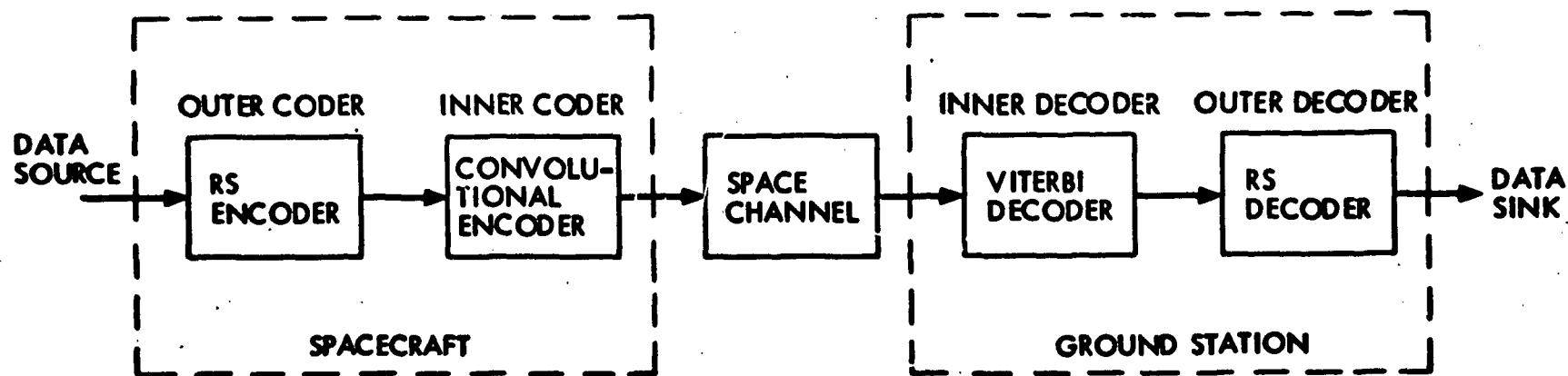
Figure 1. Concatenated Reed-Solomon/Viterbi Coding System Block Diagram

SECTION II

THE EFFECTS OF RECEIVER TRACKING PHASE ERROR ON THE PERFORMANCE OF THE CONCATENATED RS/VITERBI CODING SYSTEM

2.1 ANALYTICAL RESULTS

A block diagram of the ground receiving system, with carrier and subcarrier demodulators, symbol synchronizer, Viterbi decoder, and Reed-Soldmon decoder, such as the Deep Space Network (DSN) ground receiving system is shown in Fig. 2. The carrier tracking loop and data demodulation can be modeled as shown in Fig. 3 (Refs. 12, 13, and 14). The received IF signal r(t) (point ① in Fig. 3) is given by

$$r(t) = \sqrt{2P_T} \cos \{\omega_c t + \theta_m d(t) \sqcap \text{in} [\omega_{sc} t + \theta_{sc}(t)]\}$$

$$= \sqrt{2P_c} \sin [\omega_{IF} t + \theta_c(t)] + \sqrt{2P_D} d(t) \sqcap \text{in} [\omega_{sc} t + \theta_{sc}(t)]$$

$$\times \cos [\omega_{IF} t + \theta_c(t)] + \dot{n}(t) \qquad (1)$$

where

$P_c = P_T \cos^2\theta_m$ = carrier power

P_T = total transmitter power

θ_m = modulation index

$P_D = P_T \sin^2\theta_m$ = data power

ω_{IF} = IF carrier angular frequency

$\theta_c(t)$ = phase uncertainty in carrier reference

$d(t)$ = BPSK data, +1 or -1

$\sqcap \text{in}(\omega_{sc} t)$ = square wave subcarrier with polarity of $\sin(\omega_{sc} t) = \pm 1$

$\theta_{sc}(t)$ = phase uncertainty in subcarrier reference

$n(t)$ = white Gaussian noise process with single-sided spectral density N_0 watts/Hz.

Figure 2. Receiving System Block Diagram
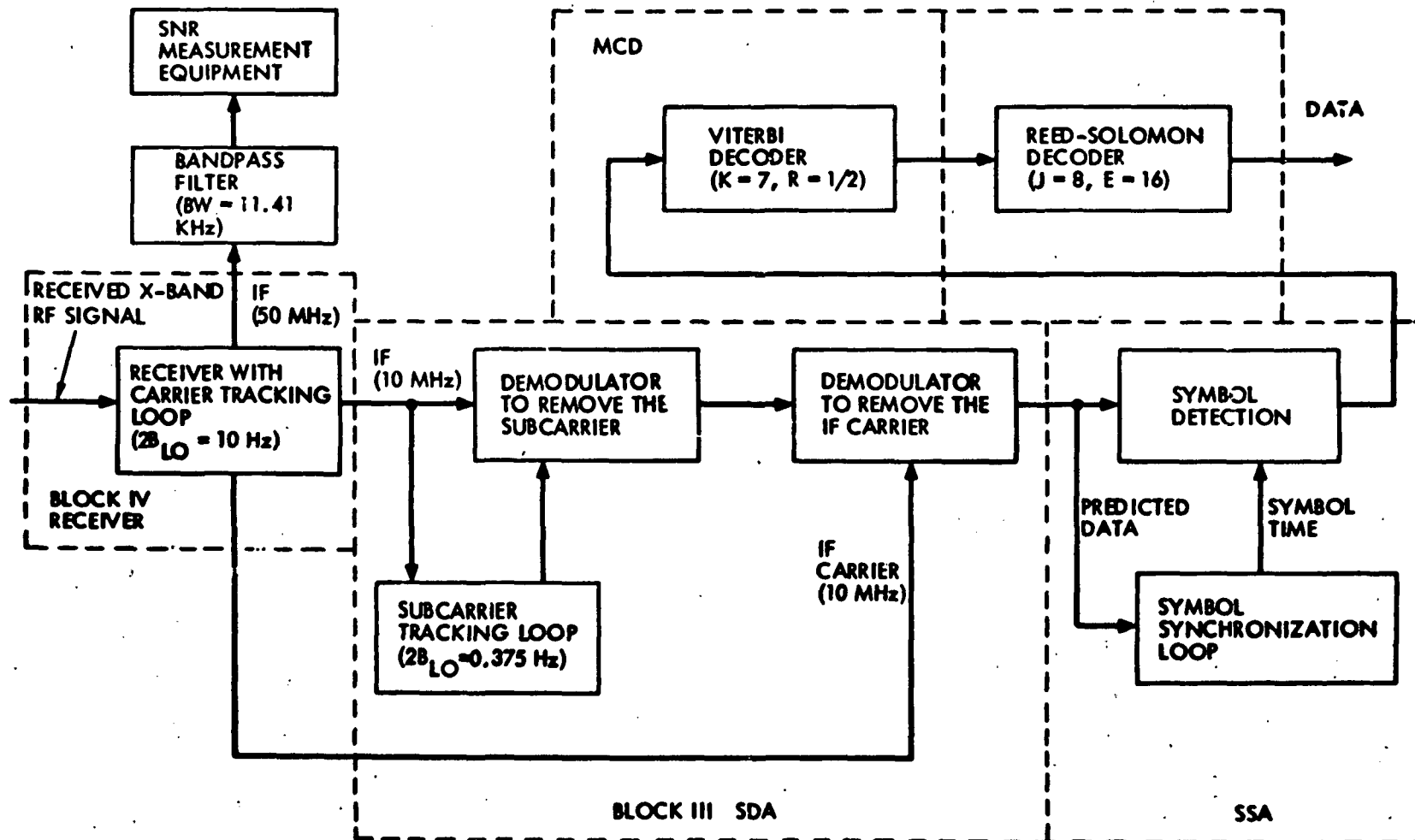
The received IF signal is mixed with the square wave subcarrier Sin $[\omega_{sc}t + \hat{\theta}_{sc}(t)]$ where $\hat{\theta}_{sc}(t)$ is the SDA estimated subcarrier phase, and then filtered by the predemodulation filter $F(s)$ to give the signal (point ③ in Fig. 3) as

$$F \{\sqrt{2P_c} \sin [\omega_{IF}t + \theta_c(t)] \mathsf{S}in [\omega_{sc}t + \hat{\theta}_{sc}(t)] +$$

$$\sqrt{2P_D} d(t) \mathsf{S}in [\omega_{sc}t + \theta_{sc}(t)] \mathsf{S}in [\omega_{sc}t + \hat{\theta}_{sc}(t)]$$

$$\cos [\omega_{IF}t + \theta_c(t)]\} + n_1(t) \tag{2}$$

where $n_1(t)$ is a white Gaussian noise process with one-sided spectral density of N_0 watts/Hz. The first term of Equation (2) is filtered out by $F(s)$, therefore the filtered signal is

$$\sqrt{2P_D} d(t) \mathsf{S}in [\omega_{sc}t + \theta_{sc}(t)] \mathsf{S}in [\omega_{sc}t + \hat{\theta}_{sc}(t)] \times$$

$$\cos [\omega_{IF}t + \theta_c(t)]\} + n_1(t) \tag{3}$$

The filtered signal at ③ is then mixed with the IF reference signal

$$\sqrt{2} \cos [\omega_{IF}t + \hat{\theta}_c(t)]$$

where $\hat{\theta}_c(t)$ is the carrier tracking loop estimated carrier phase. The resulting signal $S(t)$ (point ④ in Fig. 3) is given by

$$S(t) = \sqrt{P_D} d(t) \{\mathsf{S}in [\omega_{sc}t + \theta_{sc}(t)] \mathsf{S}in [\omega_{sc}t + \hat{\theta}_{sc}(t)]\} \times$$

$$\cos [\theta_c(t) - \hat{\theta}_c(t)] + n_2(t) \tag{4}$$

13

Since

$$\sin[\omega_{sc}t + \theta_{sc}(t)]\,\sin[\omega_{sc}t + \hat{\theta}_{sc}(t)] = 1 - \left(\frac{2}{\pi}\right)|\theta_{sc}(t) - \hat{\theta}_{sc}(t)|$$

by (4), one has the equation

$$S(t) = \sqrt{P_D}\left[1 - \left(\frac{2}{\pi}\right)|\phi_s(t)|\right]\cos\phi_c(t) + n_2(t) \qquad (5)$$

where

$\phi_s(t) = \theta_{sc}(t) - \hat{\theta}_{sc}(t) =$ phase error in the subcarrier tracking loop

$\phi_c(t) = \theta_c(t) - \hat{\theta}_c(t) =$ phase error in the carrier tracking loop

$n_2(t) =$ a white Gaussian noise process with one-sided spectral density
     of N_0 watts/Hz.

The signal $S(t)$ from the SDA is correlated with the estimated BPSK data $d[t - (i - 1)T_s - \epsilon]$, where T_s is the symbol interval and ϵ is the symbol timing error, and integrated over the symbol time. The result of the integration is dumped to the A/D converter every symbol time to provide a 3-bit soft decision data to the Viterbi decoder. The integrate-and-dump circuit output (point ⑤ in Fig. 3) is given by

$$S'(iT_s) = \frac{K}{T_s}\int_{(i-1)T_s+\epsilon}^{iT_s+\epsilon}\left\{\sqrt{P_D}\,d(t)\,d[t - (i-1)T_s - \epsilon] \times \left[1 - \left(\frac{2}{\pi}\right)|\phi_s(t)|\right] \times \cos\phi_c(t)\right\}dt + K\,n_3(iT_s)$$

$$\qquad (6)$$
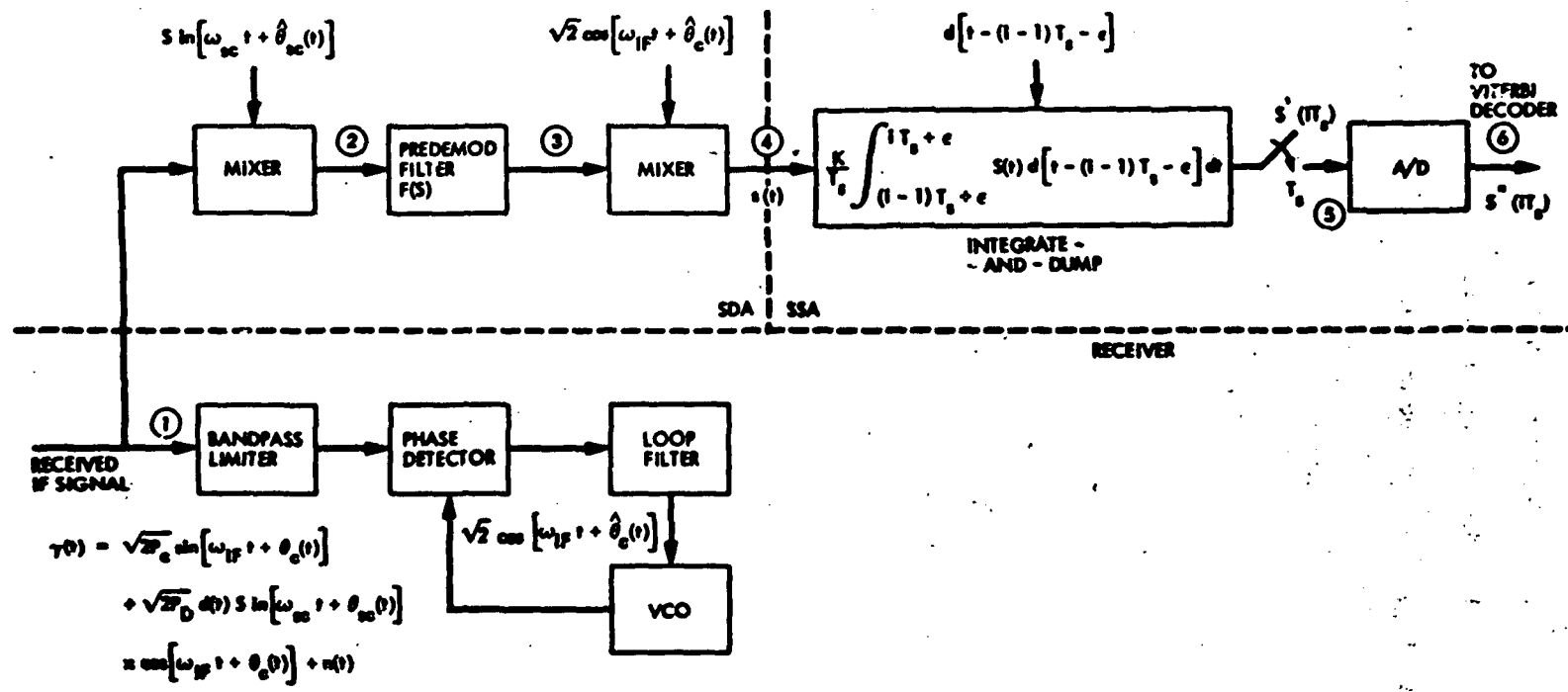
Figure 3. Carrier Tracking Loop and Data Demodulation Model

where

i = ith symbol interval

K = integrate-and-dump circuit gain

$n_3(iT_s)$ = a zero mean Gaussian random variable with

variance $\dfrac{N_0}{2T_s}$ and $n_3(iT_s)$ is independent

of $n_3(jT_s)$ for $i \neq j$.

If the gain K of the integrate-and-dump circuit is set to equal $1/\sqrt{N_0/2T_s}$ then (6) becomes

$$S'(iT_s) = \sqrt{\frac{2E_s}{N_0}} \frac{1}{T_s} \int_{(i-1)T_s+\epsilon}^{iT_s+\epsilon} \left\{ d(t)\, d[t - (i-1)\, T_s - \epsilon] \times \left[1 - \left(\frac{2}{\pi}\right) |\phi_s(t)|\right] \times \cos \phi_c(t) \right\} dt + n_4(iT_s) \tag{7}$$

where

$n_4(iT_s)$ = a zero mean unit variance Gaussian random variable

$E_s = P_D T_s$ = energy per symbol.

If the carrier and the subcarrier tracking loop bandwidths are much smaller than the symbol rate, then the terms

$$\left[1 - \left(\frac{2}{\pi}\right) |\phi_s(t)|\right]$$

16

and cos $\phi_c(t)$ in (7) can be considered as constants over the symbol interval. In this case (7) can be expressed as:

$$S'(iT_s) = \sqrt{\frac{2E_s}{N_0}} \left[1 - \left(\frac{2}{\pi}\right)|\phi_s(iT_s)| \right] \cos \phi_c(iT_s) \times$$

$$\left[\frac{1}{T_s} \int_{(i-1)T_s+\varepsilon}^{iT_s+\varepsilon} d(t) \ d\left[t - (i-1)T_s - \varepsilon \right] dt \right] + n_4(iT_s)$$

(8)

If the bandwidth of the symbol synchronizer is much smaller than the symbol rate, then the symbol reference error ε can be considered as a constant over the symbol interval. In this case

$$\frac{1}{T_s} \int_{(i-1)T_s+\varepsilon}^{iT_s+\varepsilon} d(t) \ d\left[t - (i-1)T_s - \varepsilon \right] dt = 1 - \frac{2|\varepsilon(iT_s)|}{T_s}$$

$$= 1 - 2|\lambda(iT_s)| \qquad (9)$$

where $\lambda(iT_s) = \dfrac{\varepsilon(iT_s)}{T_s}$ = normalized symbol reference error.

Thus by (9), Eq. (8) becomes

$$S'(iT_s) = \sqrt{\frac{2E_s}{N_0}} \left[1 - \left(\frac{2}{\pi}\right)|\phi_s(iT_s)| \right] \cos \phi_c(iT_s) \times \left[1 - 2|\lambda(iT_s)| \right] + n_4(iT_s)$$

(10)

17

From (10) one can see that the signal component of the matched filter output is degraded by the factor

$$\left[1 - \left(\frac{2}{\pi}\right) |\phi(iT_s)|\right] \cos \phi_c (iT_s) \left[1 - 2\lambda(iT_s)\right]$$

Suppose the bit error probability, P_e, of the Viterbi decoder under perfect carrier, subcarrier, and symbol tracking loops is given by

$$P_e = f(E_b/N_0) \tag{11}$$

where $E_b/N_0 = P_D T/N_0 =$ SNR measured at receiver 50 MHz IF. Now, if ϕ_s, ϕ_c, and λ are constants over all Viterbi decoder errors then by (10) and (11) the conditional bit error probability for constant ϕ_s, ϕ_c and λ under a perfect A/D converter is given by

$$P_e(\phi_s, \phi_c, \lambda) = f \left\{ \frac{E_b}{N_0} \left[1 - \left(\frac{2}{\pi}\right) |\phi_s|\right]^2 \cos^2 \phi_c \left[1 - 2|\lambda|\right]^2 \right\} \tag{12}$$

The bit error probability of the high-rate model is thus given by

$$P_e = \int_{-1/2}^{1/2} \int_{-\pi/2}^{\pi/2} \int_{-\pi}^{\pi} P_e(\phi_s, \phi_c, \lambda) \, p(\phi_s, \phi_c, \lambda) \, d\phi_c \, d\phi_s \, d\lambda \tag{13}$$

where $p(\phi_s, \phi_c, \lambda)$ is the joint probability of ϕ_s, ϕ_c and λ. For small carrier tracking phase error, ϕ_c, ϕ_s, and λ can be considered as statistically independent random variables. Thus $p(\phi_c, \phi_s, \lambda)$ in (13) can be expressed as

$$p(\phi_c, \phi_s, \lambda) = p(\phi_c) \, p(\phi_s) \, p(\lambda)$$

2-8

By the above equation (13) becomes

$$P_e = \int_{-1/2}^{1/2} \int_{\frac{\pi}{2}}^{\frac{\pi}{2}} \int_{-\pi}^{\pi} P_e(\phi_c, \phi_s, \lambda) \, p(\phi_c) \, p(\phi_s) \, p(\lambda) \, d\phi_c d\phi_s d\lambda \qquad (14)$$

where $p(\phi_c)$, $p(\phi_s)$, and $p(\lambda)$ are the probability densities of phase errors in the carrier, subcarrier and symbol tracking loops, respectively.

In a two-way transmission with a strong uplink, the contribution made by the phase error in the carrier tracking loop in the spacecraft to the two-way phase error can be neglected. Hence the probability density of the two-way phase error can be approximated by the probability density of the one-way phase error ϕ_c in the carrier tracking loop of the ground receiver as [Ref. 12]

$$p(\phi_c) = \frac{\exp(\rho \cos\phi_c)}{2\pi I_o(\rho)} \, , \, |\phi_c| \leq \pi \qquad (15)$$

In (15), ρ is the carrier tracking loop SNR given by

$$\rho = \frac{P_c}{N_o \times B_L \times \Gamma}$$

where

P_c = carrier power

N_o = one-sided noise spectral density in the ground receiver

B_L = one-sided carrier loop bandwidth in the ground receiver

Γ = bandpass limiter suppression factor in the ground phase-locked receiver (Ref. 15).

The phase error variance $\sigma^2_{\phi_c}$ is given by

$$\sigma^2_{\phi_c} = \frac{1}{\rho} \qquad (16)$$

In a two-way transmission with a weak uplink, the contribution made by the phase error in the carrier tracking loop in the spacecraft to the two-way phase error cannot be neglected. Hence the probability density of the two-way phase error ϕ_c should be given by (Ref. 15)

$$p(\phi_c) = \frac{I_o\left[\left(\alpha_1^2 + \rho_2^2 + 2\alpha_1 \rho_2 \cos\phi_c\right)^{1/2}\right]}{2\pi \, I_o(\rho_1) \, I_o(\rho_2)} \quad ; |\phi_c| \le \pi \qquad (17)$$

where

$$\alpha_1 = \frac{\rho_1}{G^2 K_R}$$

$$\rho_n = \frac{P_{cn}}{N_{on} B_{Ln} \Gamma_n} = \text{carrier loop SNR in the spacecraft receiver } (n = 1)$$
and the ground receiver $(n = 2)$.

P_{cn} = carrier power $(n = 1,2)$

N_{on} = one-sided noise spectral density $(n = 1,2)$

B_{Ln} = one-sided carrier loop bandwidth $(n = 1,2)$

Γ_n = bandpass limiter suppression factor $(n = 1,2)$

G = static phase gain of the spacecraft transponder = 880/221 for S-band uplink and X-band downlink

K_R = loop parameter function (Ref. 15, p. 94)

2-10

The two-way phase error variance $\sigma^2_{\phi_c}$ is given by (Ref. 15)

$$\sigma^2_{\phi_c} = \frac{1}{\alpha_1} + \frac{1}{\rho_2} = \sigma^2_{\phi_1} + \sigma^2_{\phi_2} \qquad (18)$$

where

$$\sigma^2_{\phi_1} = \frac{1}{\alpha_1} = \text{transponder turn-around phase noise}$$

A parameter, which is related to the carrier loop SNR at threshold loop bandwidth, is called the carrier margin M_{cn}. This parameter is defined as

$$M_{cn} \triangleq \frac{P_{cn}}{2B_{L_o}n N_{on}} \qquad n=1,2 \qquad (19)$$

where

$$B_{L_o}n = \text{one-sided carrier threshold loop bandwidth.}$$

The probability density function of the SDA phase error ϕ_s in (14) is given by (Ref. 15)

$$p(\phi_s) = \frac{\exp{(\rho_s \cos 2\phi_s)}}{\pi I_o(\rho_s)} \quad ; \quad |\phi_s| \leq \frac{\pi}{2}$$

where

$$\rho_s = \text{SDA loop SNR.}$$

The probability density of the normalized SSA phase error λ in (14) is given by (Ref. 15)

$$p(\lambda) = \frac{\exp{[(\cos 2\pi\lambda)/(2\pi\sigma_\lambda)^2]}}{I_o[(1/2\pi\sigma_\lambda)^2]} \quad ; \quad |\lambda| \leq 1/2$$

2-11

where

$$\sigma_\lambda^2 = \text{SSA normalized phase error variance.}$$

From (13) and (14), one can see that the system loss suffered in the demodulation of downlink data, which is determined by the extra E_b/N_0 required to achieve the same bit error rate, will be comprised of:

    (1) Losses due to imperfect carrier synchronization (the radio loss).

    (2) Losses due to imperfect subcarrier synchronization (subcarrier synchronization loss).

    (3) Losses due to imperfect bit timing (bit synchronization loss).

The residual carrier usually has much less power than the data power (e.g., the residual carrier is 15 dB below the total power of the transmitted signal for a residual index of 80°). And, since the subcarrier frequency and the data rate are both much less than the carrier frequency, the carrier loop bandwidth is normally much wider than those of the subcarrier and bit synch loops, due to dynamic considerations. As a consequence, radio loss due to carrier jitter is the dominant factor in the total system loss. Hence we will use radio loss to approximate the system loss. Letting $\phi_s = \lambda = 0$ in (12) and using (14), one has

$$P_e = \int_{-\pi}^{\pi} f\left(\frac{E_b}{N_0} \cos^2\phi_c\right) \, P(\phi_c) \, d\phi_c \qquad (20)$$

where $p(\phi_c)$ is the probability density of the receiver phase tracking error. The P_e versus E_b/N_0 curves for different loop SNR's in a one-way communication and for different uplink carrier margins with a fixed downlink carrier loop SNR of 13.5 dB in a two-way communication are shown in Figs. 4 and 5, respectively for a $K = 7$, $R = 1/2$ Viterbi-coded convolutional code.

22
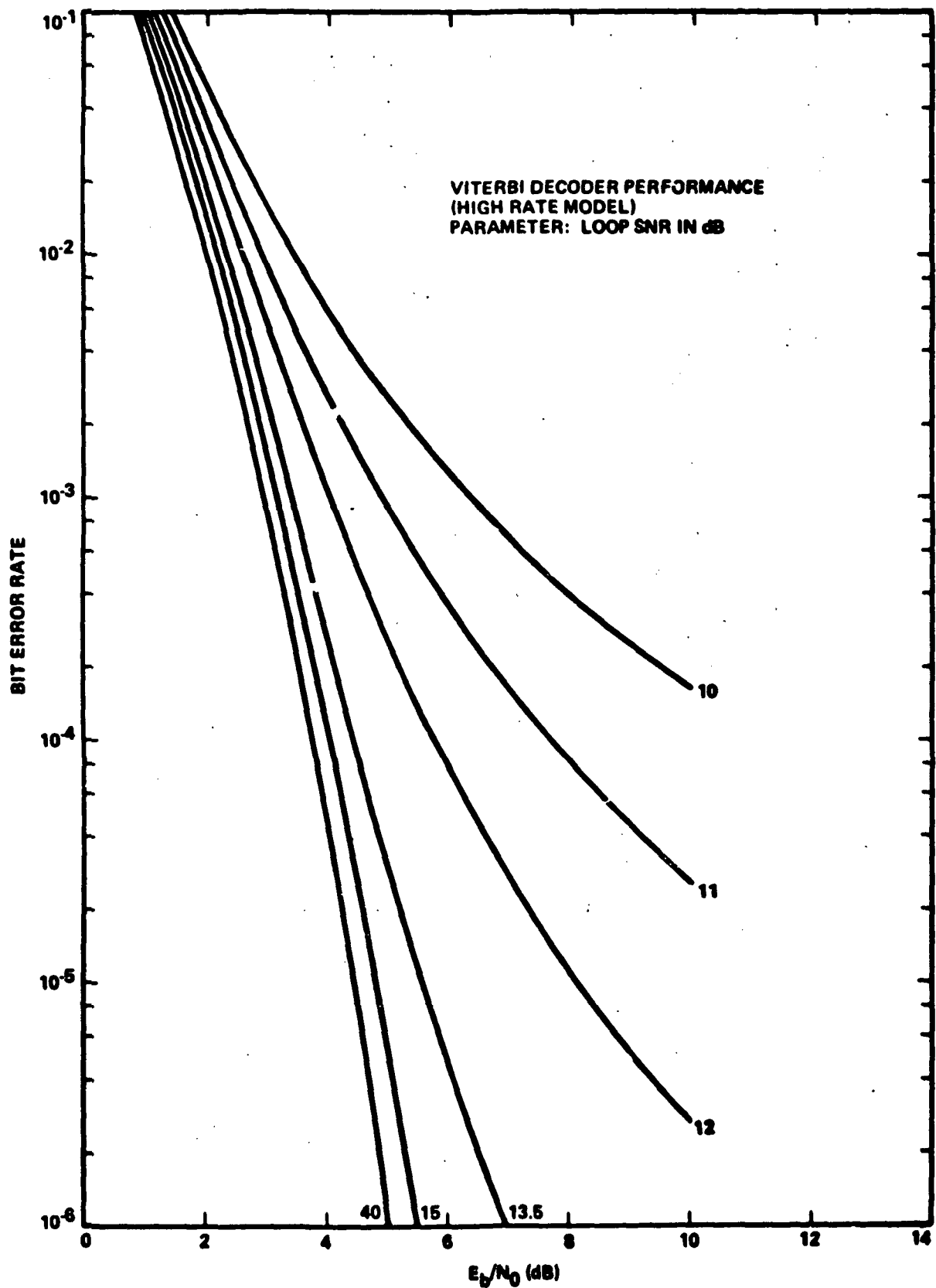
Figure 4. Viterbi Decoder Bit Error Rate Vs. Carrier Loop SNR (High Rate Model)

23
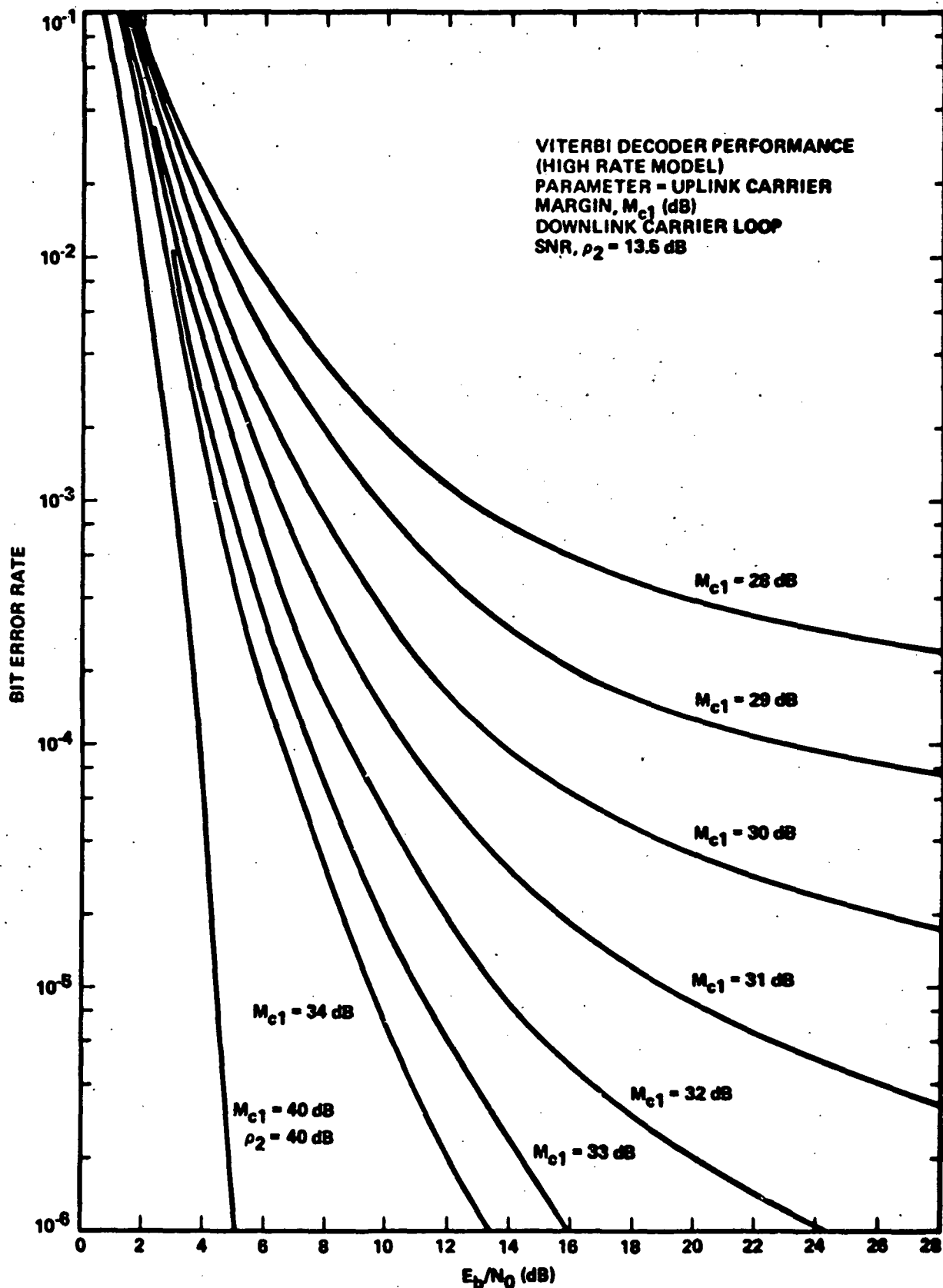
Figure 5. Viterbi Decoder Performance for Weak Uplink/Weak Downlink
(High Rate Model).

An error burst on the Viterbi decoder output is defined as a sequence of decoded bits that begins with a bit in error, ends with a bit in error, and has fewer than K-1 correct bits within the burst. The measurement results (Ref. 18) showed that the average error burst length and the probability of bit error within a burst of a K=7 Viterbi decoder did not vary too much over a wide range of BER's from 10^{-3} to 10^{-7}. Therefore, it is reasonable to assume that the average number of bit errors in an RS symbol error is a constant.

Using the above assumption, the bit error probability (BEP) P_b at the RS decoder output can be expressed as:

$$P_b = \frac{P_e \times P_{SO}}{P_{SI}} \qquad (21)$$

where P_{SI} and P_{SO} are the symbol error probabilities (SEP) at the RS decoder input and output, respectively. Let the symbol error probability of the Viterbi decoder for an ideal receiver be given by $g(E_b/N_o)$. Then the symbol error probability for a constant carrier phase error ϕ_c can be expressed as

$$g\left(\frac{E_b}{N_o} \cos^2\phi_c\right)$$

Thus, the symbol error probability for a non-ideal receiver can be obtained as (Ref. 7).

$$P_{SI} = \int_{-\pi}^{\pi} g\left(\frac{E_b}{N_o} \cos^2\phi_c\right) p(\phi_c) \, d\phi_c \qquad (22)$$

Let E be the number of symbols an RS code is able to correct. Then for a perfectly interleaved system P_{SO} is equal to

2-13

$$P_{SO} = \sum_{i=E+1}^{2^J-1} \left(\frac{i}{2^J-1}\right) \binom{2^J-1}{i} P_{SI}^{i}(1-P_{SI})^{2^J-1-i} \qquad (23)$$

where (2^J-1) is the number of symbols in an RS codeword. By (22) and (23), the bit error probability P_b of the concatenated system given in (21) is equal to

$$P_b = P_e \sum_{i=E+1}^{2^J-1} \left(\frac{i}{2^J-1}\right) \binom{2^J-1}{i} P_{SI}^{i-1} (1-P_{SI})^{2^J-1-i} \qquad (24)$$

For a perfectly interleaved system the RS word error probability (WEP) P_w is given by (Ref. 3).

$$P_w = \sum_{i=E+1}^{2^J-1} \binom{2^J-1}{i} (P_{SI})^{i} (1-P_{SI})^{2^J-1-i} \qquad (25)$$

Thus once the bit and symbol error probabilities of the Viterbi decoder output are obtained, the bit, symbol, and word error probabilities of the concatenated system can then be determined by computing (23), (24), and (25). The one-way and two-way radio loss curves as a function of carrier jitter and Viterbi decoder input bit signal-to-noise ratio for a concatenated $J = 8$, $E = 16$ perfectly interleaved RS code and a $K = 7$, $R = 1/2$ Viterbi-decoded convolutional code are shown in Figures 6 and 7, respectively. The Viterbi decoder output symbol error probability $g(E_b/N_o)$ used in obtaining the one-way and two-way radio loss curves, is taken from the simulation data.

26
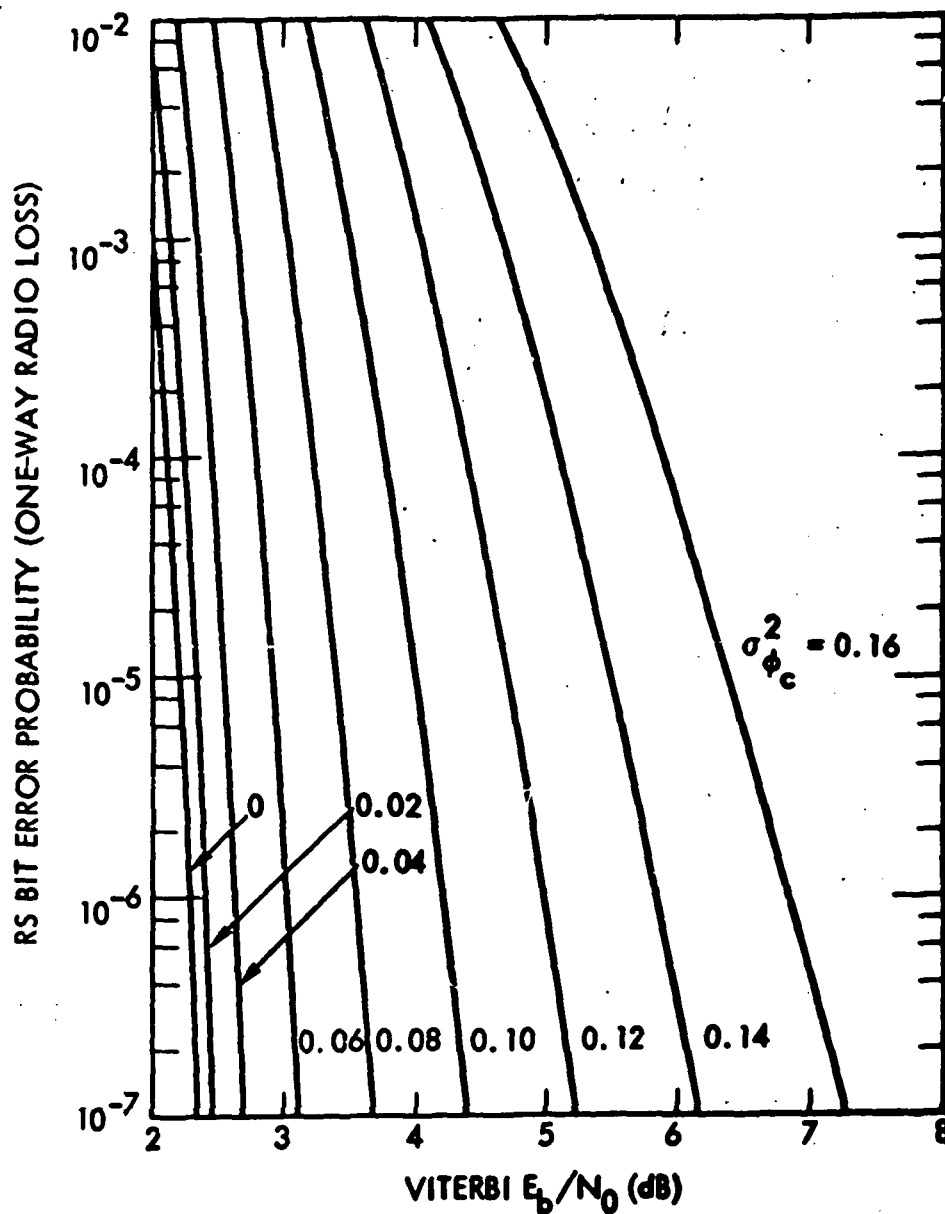
Figure 6. Concatenated Code Performance with One Way Radio Loss, Given as Functions of Receiver Phase Lock Loop Carrier Jitter (Radian^2) for Perfect Interleaving.

27
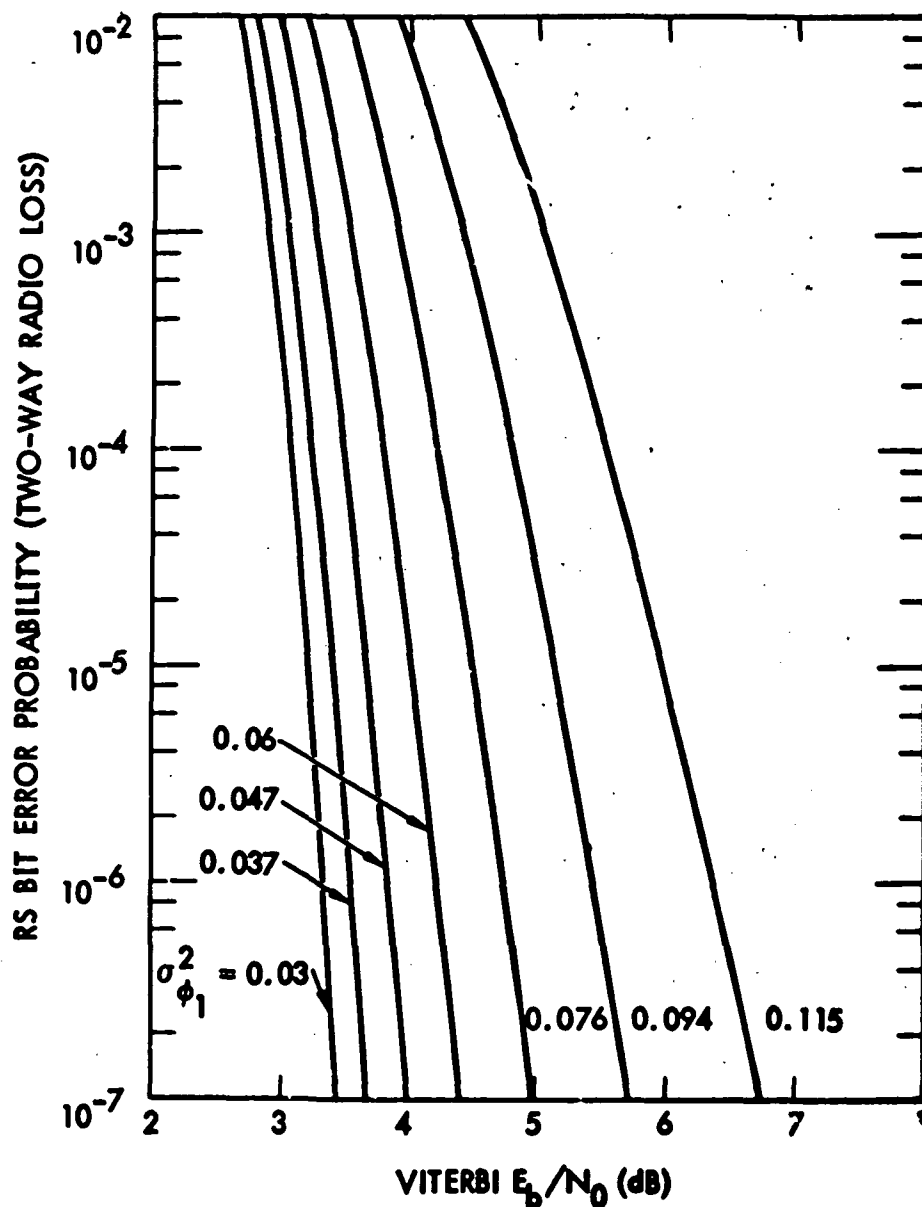
Figure 7. Concatenated Code Performance with Two-Way Radio Losses, Given as a Function of Transponder Turn-Around Phase Noise (Radian^2) with Down-Link Loop SNR = 13.5 dB (i.e., $\sigma^2_{\phi_2}$ = 0.045 radian^2) for Perfect Interleaving.

2-18

28

The performance obtained using the above assumptions of a perfect interleaving and a constant bit error per RS input error symbol is useful for system tradeoffs study. However, for actual system design one has to rely on the experimental method to obtain realistic system performance for various interleaving depths.

This section describes the objectives of such an experiment, its setup, and the results obtained. This experiment has been performed utilizing the TDL facilities.

2.2 TEST OBJECTIVES

The test objectives of this experiment are:

(1) To determine the bit and word error probabilities of the Viterbi-decoded convolutional-only coding system and the RS/Viterbi coding system under an emulated two-way transmission with weak carrier power on either the uplink or the downlink or both.

(2) To compare the coding gains of the RS/Viterbi coding system with the Viterbi-decoded convolutional-only coding system.

(3) To test the sensitivities of the factors which affect the RS/Viterbi coding system performance such as the interleaving depth, convolutional code synchronization, etc.

2.3 TEST PARAMETERS AND ENVIRONMENT

Test parameters and environment are as follows:

(1) Test data rates = 4 to 20 kbits/second.

(2) A K = 7, rate (R) = 1/2 Viterbi-decoded convolutional code is concatenated with a J = 8, E = 16 RS code, where J is the number of bits in each RS symbol and E is the maximum number of correctable RS symbols.

2-19

(3) Interleaving level (I) = 1, 2, 4, 8, and 16.

(4) S-band uplink and X-band downlink two-way transmission through a transponder. One-way transmission is emulated by a two-way transmission with a strong uplink.

(5) Transponder: NVM second-order phase-locked loop with 18 Hz threshold loop bandwidth $(2B_{LO})$.

(6) Receiver (carrier tracking loop): BLOCK IV second-order phase-locked loop with 10 Hz threshold loop bandwidth $(2B_{LO})$.

(7) SDA (subcarrier tracking loop): BLOCK III second-order Costas loop with 0.375 Hz threshold loop bandwidth $(2B_{LO})$.

(8) SSA (symbol tracking loop): second-order digital data transition tracking loop with 0.005 nominal relative loop noise bandwidth $(2B_L T)$.

(9) Telemetry subcarrier frequency: 370 kHz.

(10) Modulation index varies from 80 to 85°.

(11) Noise bandwidth used in measuring the receiver input SNR: 11410.02313 Hz.

(12) Test record size: 32640 bits (= 16 RS words).

(13) Test duration: $\geq 5 \times 10^7$ bits.

2.4 TEST SET-UP

The flow diagram of the test setup is shown in Fig. 8. It is used to emulate the concatenated RS/Viterbi coding system as well as the Viterbi decoded convolutional coding system.

2.4.1 Viterbi-Decoded Convolutional Coding System

The test source data are generated by a 2047-bit PN sequence generator and then encoded by a K = 7, R = 1/2 convolutional coder. The encoded data are

30

modulated onto the subcarrier first and then onto X-band carrier. The carrier reference is derived from an S-band uplink signal. The resulting X-band downlink RF signal is attenuated to emulate the space transmission loss and then received by the carrier tracking loop of the ground receiver.

The input E_b/N_0 is measured at the receiver 50 MHz IF. The receiver output signal is subcarrier-demodulated, symbol-synchronized, and Viterbi-decoded to reconstruct the input PN source data. The reconstructed data are then compared with the delayed PN data to generate a string of bit error patterns. This bit string is divided into 32640-bit (16 RS words) blocks and recorded on a 9-track 800 bpi tape. This string of bit error pattern essentially characterizes the Viterbi decoded convolutional coding channel.

2.4.2 RS/Viterbi Concatenated Coding System

The concatenated RS/Viterbi coding system is formed by concatenating an outer RS code of interleaving depth I with a Viterbi-decoded inner convolutional code. The test source data are encoded by a software RS coder with J = 8 and E = 16. A set of various interleaving depths (i.e., I = 2, 4, 8 and 16) are used. Each set of RS coded data are then EXCLUSIVE-OR added with the bit string stored in the error pattern tape. The resulting data simulates the input to a ground receiving station. This set of data are then de-interleaved and decoded by a software RS decoder. A comparison is subsequently made between the test source and the decoded data to determine the bit, the symbol, and the word error probabilities of the concatenated coding system. An RS codeword error is declared if more than 16 symbol errors occurred in an RS codeword.

The interleaving scheme used for the RS code is the type B interleaving as described in Ref. 4. This interleaving scheme is illustrated by an I-level interleaved RS code array as follows:

	Information Symbols	Check Symbols
Codeword No. 1	$S_1, S_{I+1} \ldots \ldots, S_{222I+1},$	$P_1^1, P_2^I \ldots \ldots \ldots, P_{32}^1$
Codeword No. 2	$S_2, S_{I+1} \ldots \ldots, S_{222I+2},$	$P_1^2, P_2^2 \ldots \ldots \ldots, P_{32}^2$
$\vdots$	$\vdots$	$\vdots$
Codeword No. I	$S_I, S_{2I} \ldots \ldots, S_{223I},$	$P_1^I, P_2^I \ldots \ldots \ldots, P_{32}^I$

Each RS code array consists of I RS codewords. The order of symbol transmission is as follows:

$$S_1, S_2 \ldots, S_I, S_{I+1}, S_{I+2}, \ldots, S_{2I}, \ldots, S_{222I+1}, S_{222I+2}, \ldots, S_{223I},$$

$$P_1^1, \ldots, P_1^I, P_2^1, \ldots, P_2^I, \ldots, P_{32}^1 \ldots, P_{32}^I$$

The de-interleaving process is the reverse of the interleaving process. The transmitted symbol sequence is reassembled during the de-interleaving process into an RS code array, and decoding is performed on each RS codeword in the array. The advantage of this interleaving scheme is that data symbols are transmitted in their natural order. Hence, the data received by the receiver can be used for real time analysis without any preprocessing. Another advantage of this interleaving scheme is the elimination of memory needed to buffer information symbols at the encoder.
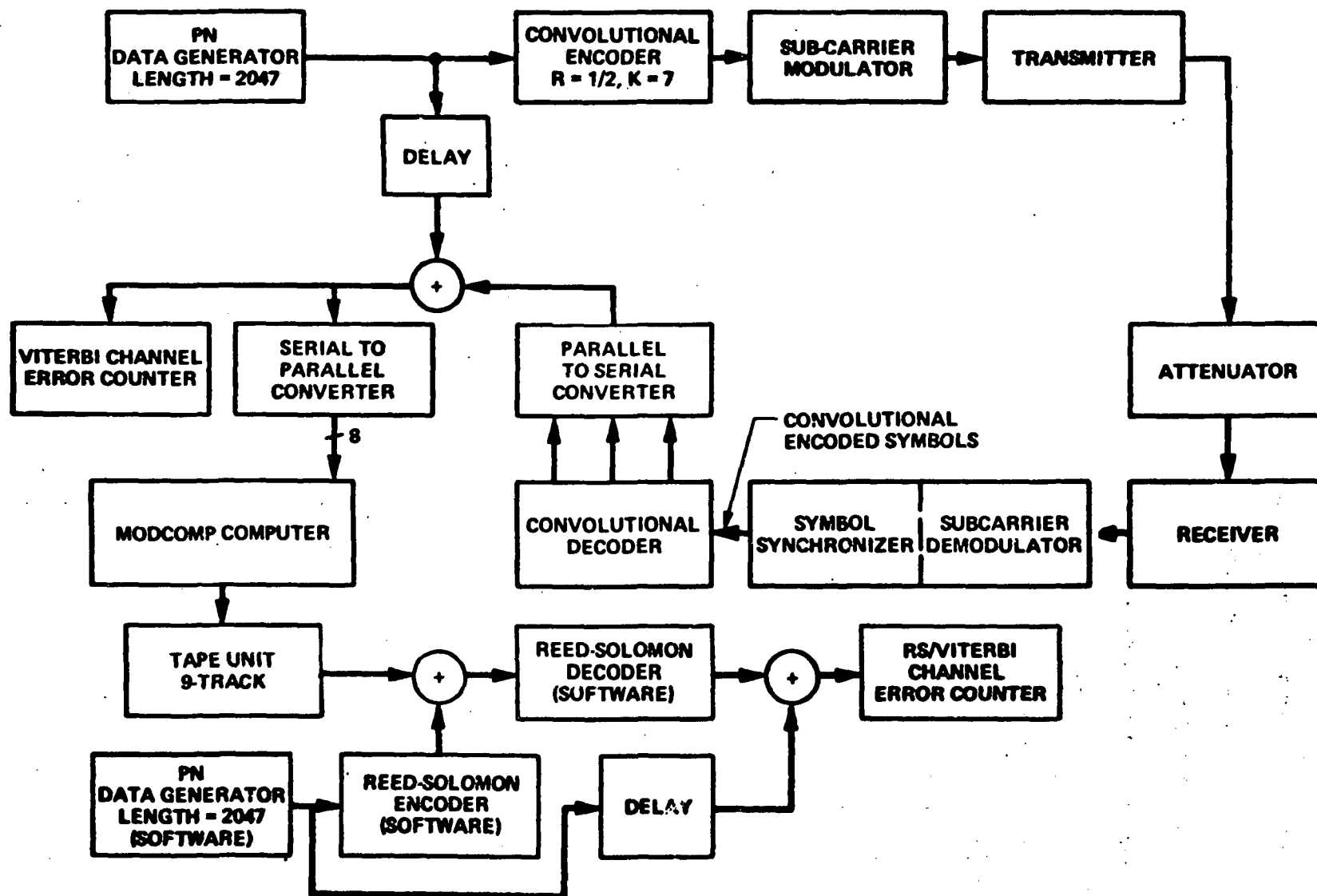
Figure 8. Test Set-Up.

2.5 TEST RESULTS

Performance tests were made in the TDL facilities to determine the performance of the Viterbi-decoded convolutional-only coding system and the RS/Viterbi coding system under an emulated S-band uplink and X-band downlink condition. A LINKABIT LV7035 Viterbi decoder is concatenated with a software $J = 8$, $E = 16$, RS decoder. The interleaving scheme used for the RS code is the type B interleaving discussed in Section 2.4. The test data rate is from 4 kHz to 20 kHz. The uplink carrier margin M_{c1} and downlink carrier loop SNR ρ_2 are carefully calibrated by varying the modulation index, the data rate, and the transmitting and receiving power. The one-way transmission is emulated by a two-way transmission with a strong uplink (uplink carrier margin = 75 dB).

The receiving system used in the tests is almost identical to the one used in a DSN ground station. The receiver carrier loop SNR versus downlink carrier margin for this particular receiving system is shown in Table 1. The variance of the two-way phase error for different uplink and downlink carrier margins, $M_{cn}(n = 1,2)$, of the particular transmitting and receiving system used in the tests are shown in Table 2. Test results for one-way and two-way radio loss are plotted in Figs. 9 to 14 as a function of carrier jitter and bit signal-to-noise ratio. An overhead of 0.6 dB is added to the E_b/N_0 required by the RS/Viterbi coding system to account for the 12.54 percent redundancy in the RS check symbols. The test results are close to the analytical prediction to within 0.5 dB for the ideal interleaving case.

34

Table 1. Block IV X-Band Receiver Carrier Loop SNR Versus
Downlink Carrier Margin

Downlink Carrier Margin $\frac{P_c}{N_0 2B_{LO}}$ (dB)	Loop Bandwidth B_L (Hz)	Carrier Loop SNR $\rho = \frac{P_c}{N_0 B_L \Gamma}$ (dB)
12.0	14.6956	9.8284
12.5	15.4349	10.1143
13	16.2122	10.3999
13.5	17.0285	10.6854
14	17.8849	10.9711
14.5	18.7823	11.2571
15	19.7215	11.5438
15.5	20.7031	11.8313
16	21.7273	12.1199
16.5	22.7939	12.4100
17	23.9025	12.7019
17.5	25.0522	12.9960
18	26.2414	13.2926
18.5	27.4682	13.5921
19	28.7296	13.8951
19.5	30.0223	14.2021
20	31.3417	14.5136
20.5	32.6828	14.8302
21	34.0395	15.1525
21.5	35.4046	15.4813
22	36.7703	15.8172
22.5	38.1279	16.1609
23	39.4680	16.5133
23.5	40.7808	16.8751
24	42.0563	17.2471

35

Table 2. Two-Way Phase Error Variance $\sigma^2_{\phi_c}$ for S-Band Uplink and X-Band Downlink

Threshold Damping Ratios ξ_n (n = 1,2)	Uplink Carrier Margin M_{c1} (dBm)	Static Phase Gain of the Transponder G	Loop Parameter Function K_R	Uplink Carrier Loop SNR ρ_1 (dB)	Downlink Carrier Margin M_{c_2} (dB)	Downlink Carrier Loop SNR ρ_2 (dB)	Two-Way Phase Error Variance $\sigma^2_{\phi_c}$
0.707	28	3.8919	0.794055	20.1868	18.5	13.5	0.159
0.707	29	3.8919	0.799449	21.0989	18.5	13.5	0.138
0.707	30	3.8919	0.803509	22.0492	18.5	13.5	0.12
0.707	31	3.8919	0.806504	23.0255	18.5	13.5	0.105
0.707	32	3.8919	0.808699	24.0149	18.5	13.5	0.092
0.707	33	3.8919	0.810319	25.0082	18.5	13.5	0.082
0.707	34	3.8919	0.811533	26.0021	18.5	13.5	0.075

From the measured two-way Viterbi decoder radio loss curves, one can see that the measured curves diverge from the theoretical two-way high-rate radio loss curves around $E_b/N_0 = 11.5$ dB. This is because data rate becomes so low (≤ 2.5 kHz) that the high-rate radio loss model is no longer applicable. From Figures 9 to 14, one can see that the concatenated RS/Viterbi coding system with an ideal interleaving has coding gains ranging from 3 to 13 dB, at very low error probabilities ($\leq 10^{-6}$), over the Viterbi-decoded convolutional-only coding system. Also shown is that an ideal interleaving in the concatenated RS/Viterbi coding system is one with depth greater than or equal to 4.

One important aspect of the concatenated RS/Viterbi code performance is the node synchronization problem in the Viterbi decoder. If the E_b/N_0 on the Viterbi decoder is too low, then the Viterbi decoder may lose its node synchronization. The node resynchronization process may take a large number of bit periods. Consequently, large interleaving levels are required to spread out the long bursts generated by this resynchronization process. Hence to avoid using large interleaving levels in the concatenated RS/Viterbi system, the Viterbi decoder should be operated above the resynchronization threshold. In the test, the node synchronization of the Viterbi decoder is monitored. It is noted that the Viterbi decoder is operated under perfect node synchronization. Therefore, an interleaving level of 4 is very close to an ideal interleaving.

In space communications, the science data and compressed imaging data usually require very low bit probabilities ($\leq 10^{-6}$) in transmission (Refs. 4 and 10). Now if the Viterbi-decoded convolutional-only coding system is used in the space flight missions, then it is impossible to perform high-rate data transmission when weak signal conditions exist on both the uplink and the downlink. One has to perform one-way data transmission and two-way ranging or doppler measurements separately in time. Since the RS/Viterbi coding system has large coding gains

37

over the Viterbi-decoded convolutional-only coding system in two-way communication, one can alleviate the above problem by using the RS/Viterbi coding system in space flight missions. In one-way communication, because the RS/Viterbi coding system also has large coding gains over the Viterbi-decoded convolutional-only coding system, using the former coding scheme will provide more data rate protection than the latter.

THEORETICAL VITERBI DECODER
PERFORMANCE OF K=7, R=1/2
FOR CARRIER LOOP SNR = 13.5 dB
(HIGH RATE MODEL)

MEASURED RS/VITERBI
CODE PERFORMANCE

△ INTERLEAVING LEVEL = 1
○ INTERLEAVING LEVEL = 2
◇ INTERLEAVING LEVEL = 4
◉ INTERLEAVING LEVEL = 8
□ INTERLEAVING LEVEL = 16

CARRIER LOOP SNR, $\rho_2 = 13.5$ dB

$\sigma_{\phi_2}^2 = 0.079$ RADIAN^2

THEORETICAL VITERBI DECODER
PERFORMANCE OF K=7, R=1/2
FOR CARRIER LOOP SNR = 40 dB

RS BIT ERROR PROBABILITY, CONCATENATED SYSTEM
BIT ERROR PROBABILITY, VITERBI DECODER

CONCATENATED, E_b/N_0 (dB)

Figure 9. One-Way RS/Viterbi Concatenated Code Performance
($\rho_2 = 13.5$ dB, $\sigma_{\phi_2}^2 = 0.045$ radian^2)

2-29

39
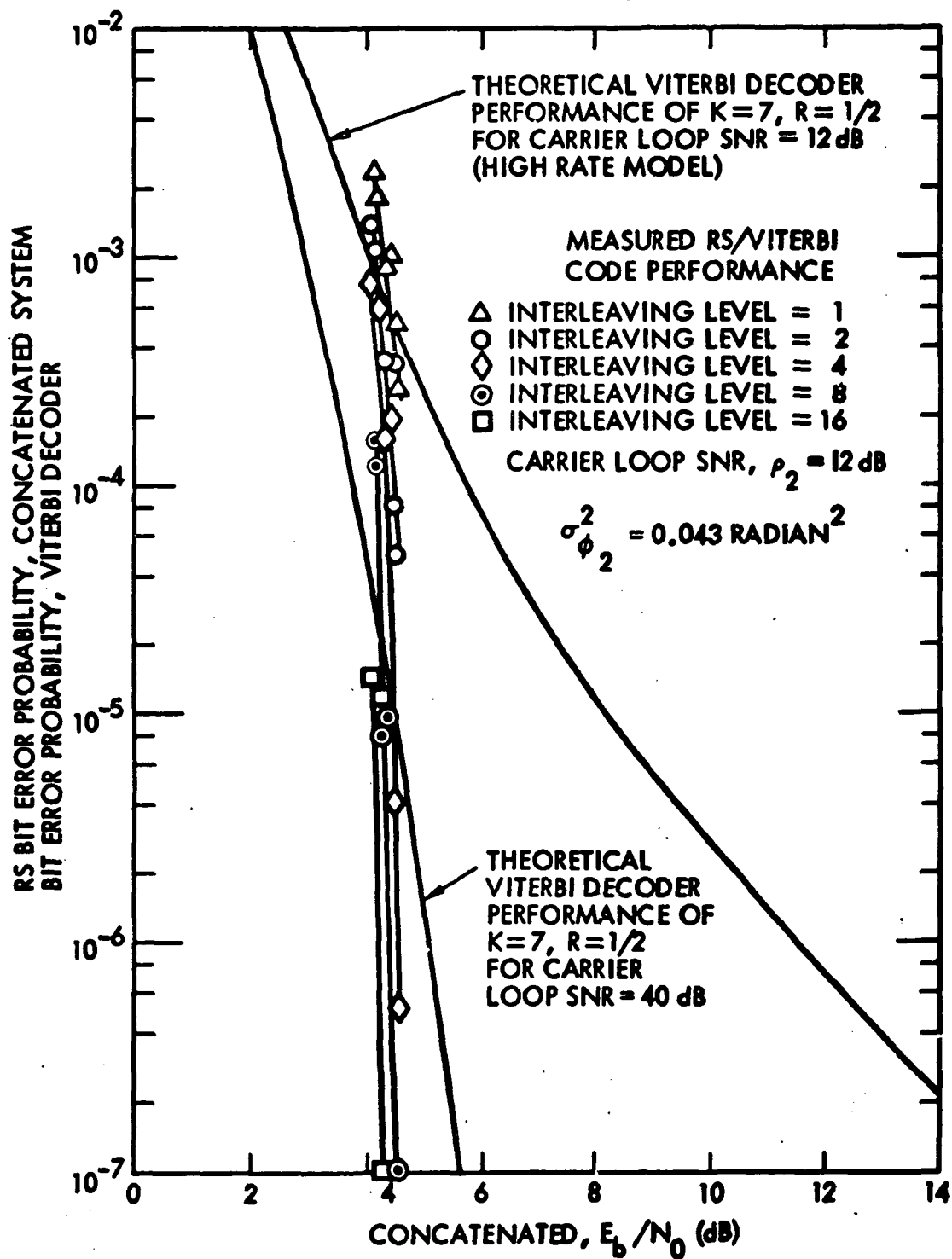
Figure 10. One-Way RS/Viterbi Concatenated Code Performance
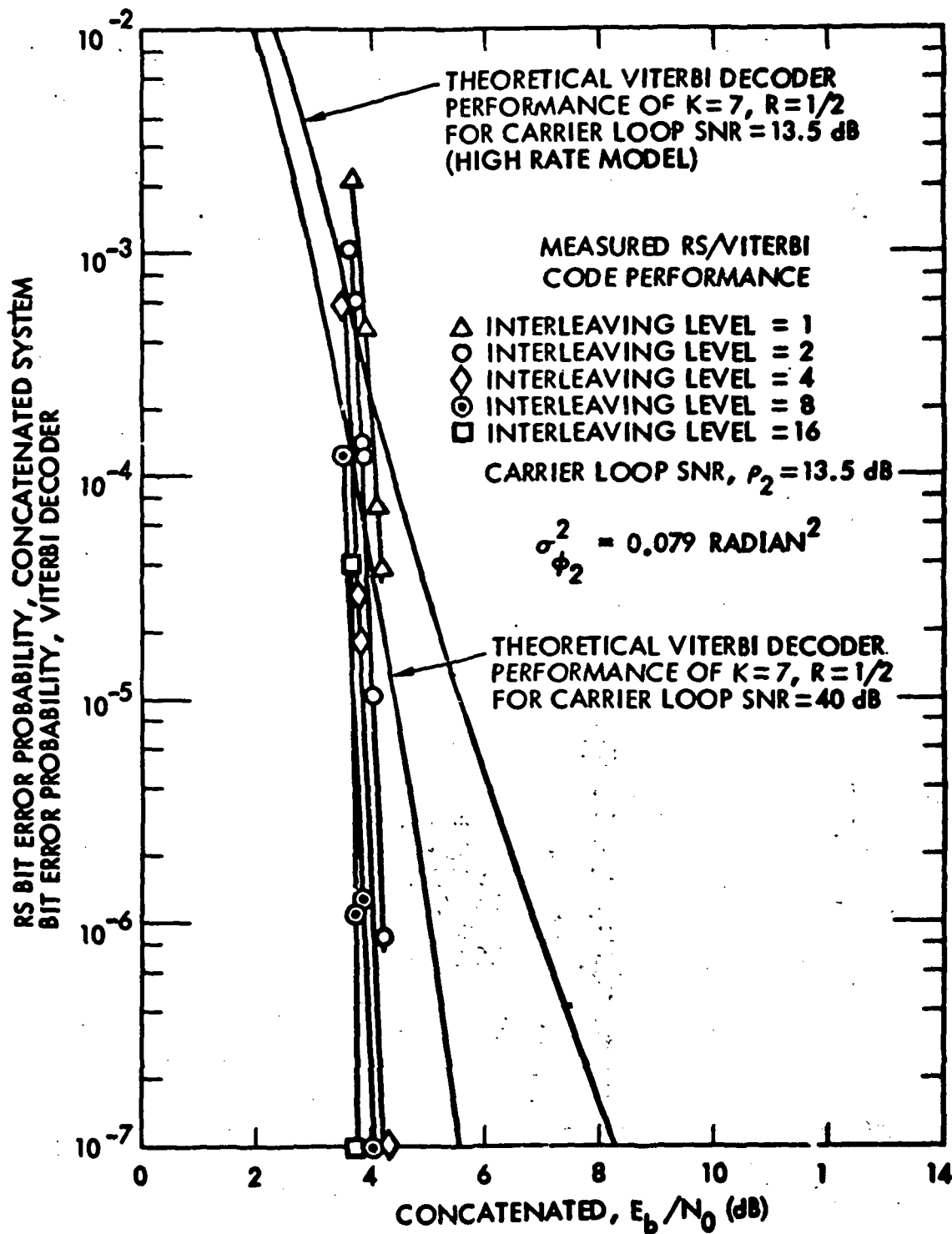(ρ_2 = 12 dB, $\sigma^2_{\phi_2}$ = 0.043 radian^2).

2-30

40
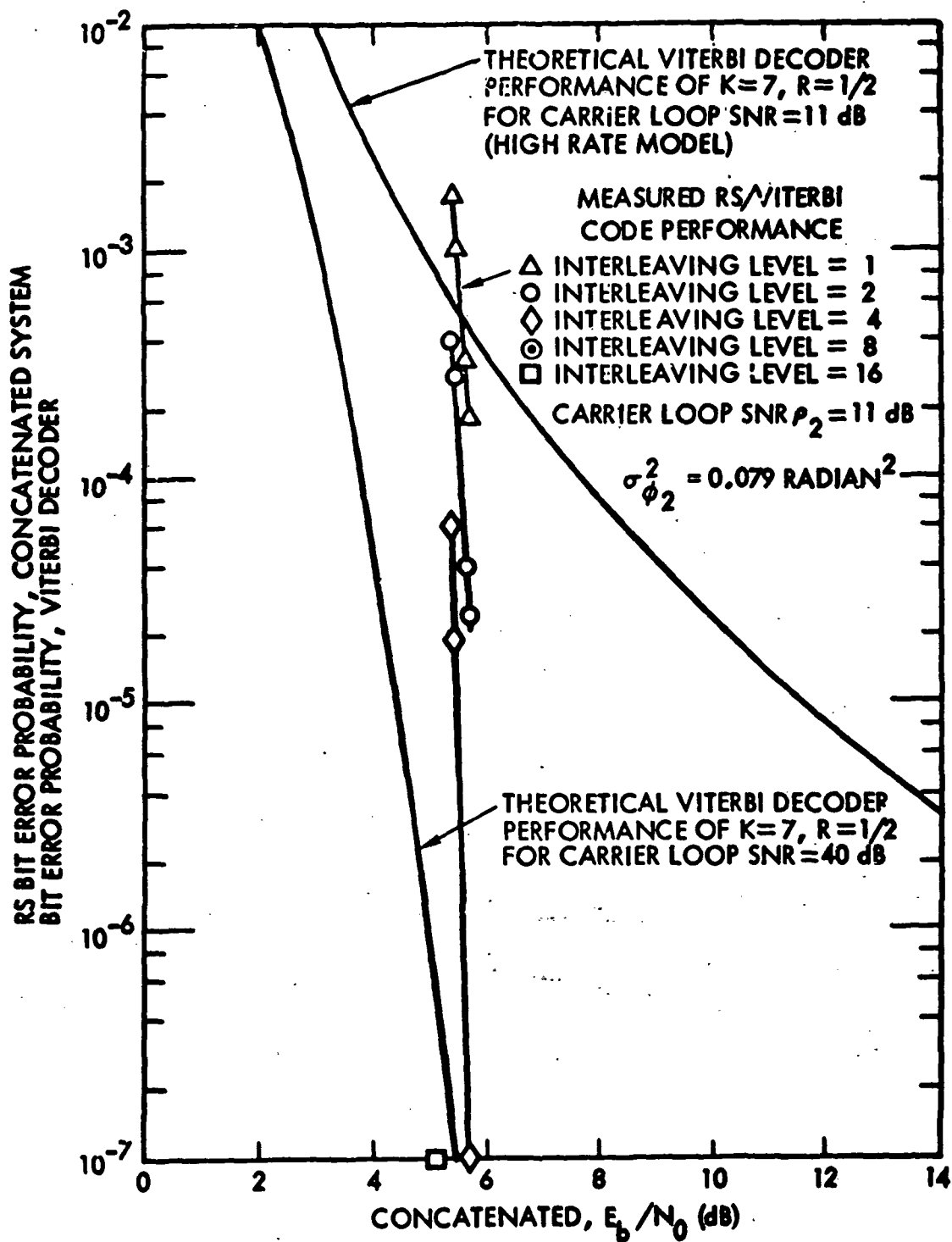
Figure 11. One-Way RS/Viterbi Concatenated Code Performance
(ρ_2 = 11 dB, $\sigma^2_{\phi_2}$ = 0.079 radian²).

2-31

41

Figure 12. RS/Viterbi Concatenated Code Performance (M_{c1} = 31 dB, ρ_2 = 13.5 dB, $\sigma_{\phi_1}^2$ = 0.06 radian^2, $\sigma_{\phi_2}^2$ = 0.045 radian^2).

Figure 13. RS/Viterbi Concatenated Code Performance (M_{c1} = 30 dB, ρ_2 = 13.5 dB, $\sigma^2_{\phi_1}$ = 0.076 radian^2, $\sigma^2_{\phi_2}$ = 0.045 radian^2)

Figure 14. RS/Viterbi Concatenated Code Performance (M_{c1} = 29 dB, ρ_2 = 13.5 dB, $\sigma^2_{\phi_1}$ = 0.094 radian², $\sigma^2_{\phi_2}$ = 0.045 radian²)
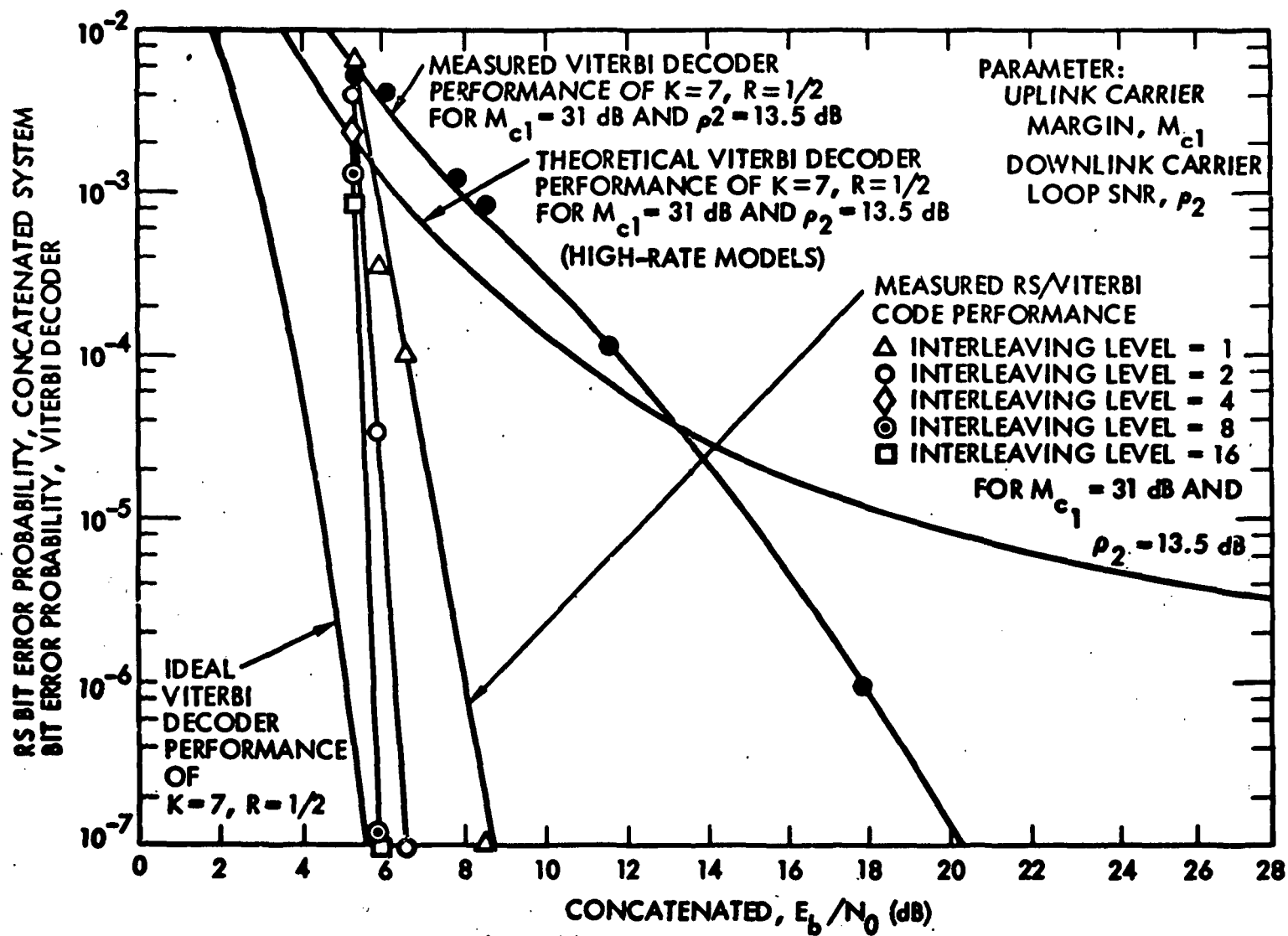
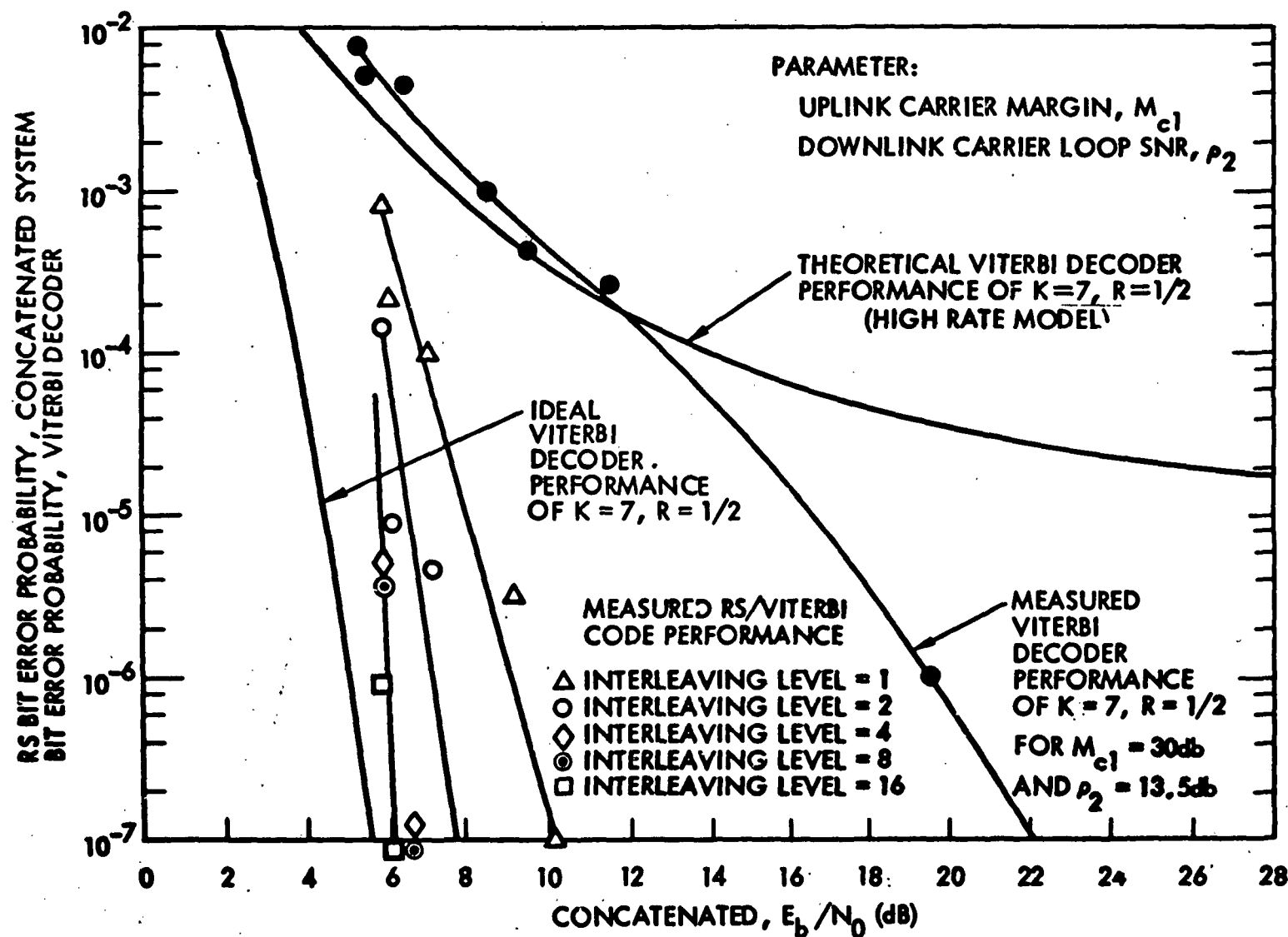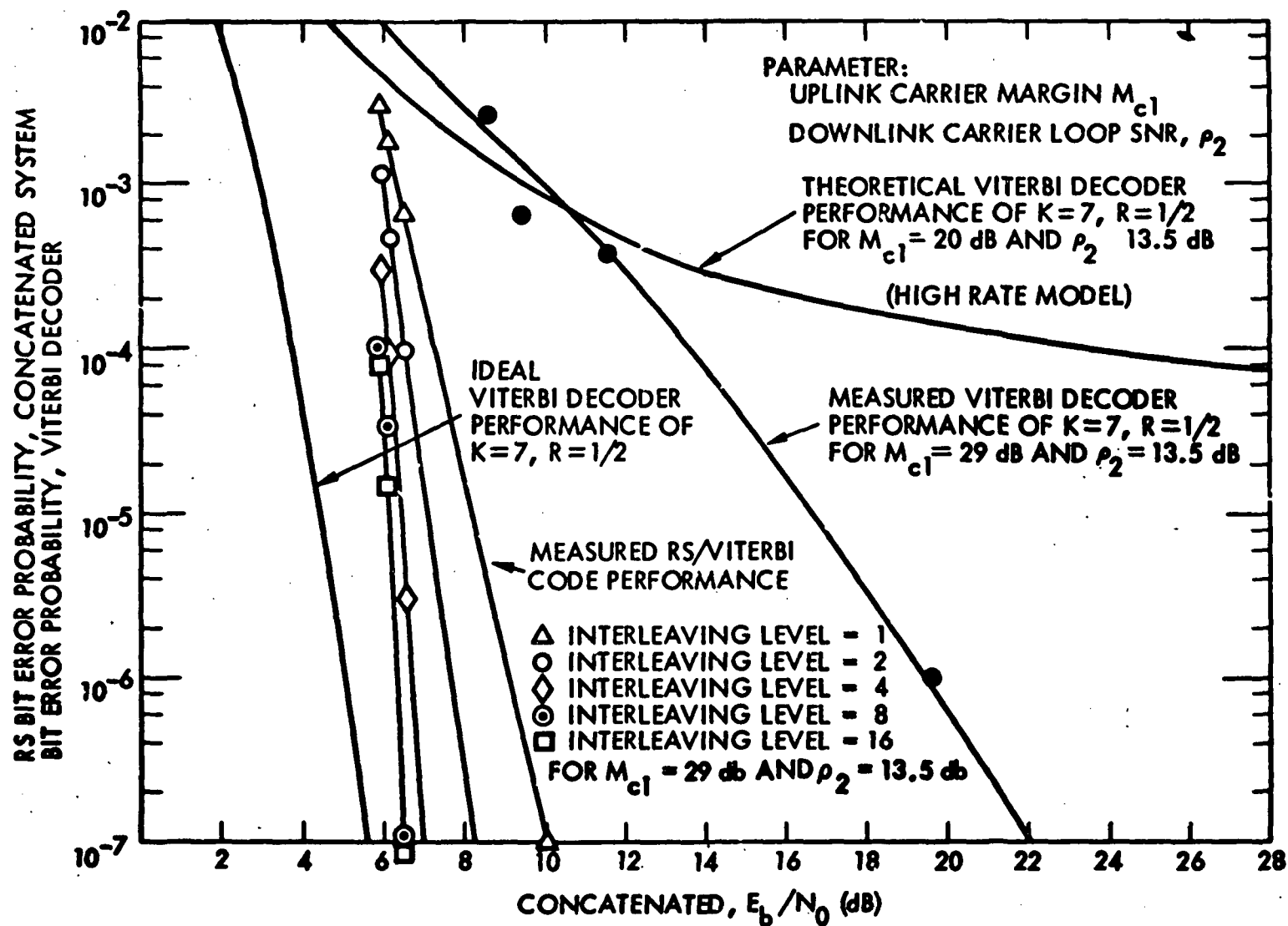EFFECTS OF RECEIVER TRACKING PHASE ERRORS ON THE CONCATENATED
RS/VITERBI CHANNEL CODING SYSTEM WITH ARRAY COMBINING

3.1 PERFORMANCE ANALYSIS

A simplified functional block diagram of an antenna array combining sys-
tem is shown in Fig. 15. The baseband signal from each receiver in the array is
a squarewave subcarrier modulated by the telemetry data. These baseband signals
are delay-adjusted by each individual tracking loops and weight-summed in the
Baseband Combiner (Refs. 16 and 17). The combiner output is fed into the Sub-
carrier Demodulator Assembly (SDA). The output of the SDA is input to the Symbol
Synchronizer Assembly (SSA) and then decoded by the Viterbi and Reed-Solomon de-
coder. The IF signal $r_i(t)$ from receiver number i ($1 \le i \le n$), where n is the
total number of receivers in the array, can be expressed as

$$r_i(t) = \sqrt{2P_{C_i}} \sin\left[\omega_{IF}t + \theta_c(t)\right] + \sqrt{2P_{D_i}} \, d(t) \, x$$

$$\sin\left[\omega_{SC}t + \theta_{SC}(t)\right] \cos\left[\omega_{IF}t + \theta_c(t)\right] + n_i(t)$$

where

P_{C_i} = carrier power in receiver i.

P_{D_i} = data power in receiver i.

ω_{IF} = IF carrier angular frequency.

$\theta_c(t)$ = phase uncertainty in carrier reference.

$d(t)$ = BPSK data, +1 or -1.

45

$\boxed{5} in(\omega_{SC}t)$ = square wave subcarrier with the polarity of $\sin(\omega_{SC}t) = \pm 1$.

$\theta_{SC}(t)$ = phase uncertainty in subcarrier reference.

$n_i(t)$ = white Gaussian noise process with single-sided spectral density N_{oi} in Watts/Hz.

The signal $r_i(t)$ is mixed with the signal $\sqrt{2}\cos\left[\omega_{IF}t + \hat{\theta}_{c_i}(t)\right]$ where $\hat{\theta}_{c_i}(t)$ is the carrier tracking loop estimated carrier phase in receiver i, and filtered to give the baseband signal $r_i'(t)$ as

$$r_i'(t) = \sqrt{P_{D_i}}\, d(t)\, \boxed{5} in\left[\omega_{SC}t + \theta_{SC}(t)\right]\cos\phi_{c_i}(t) + n_i'(t) \qquad (26)$$

where

$$\phi_{c_i}(t) = \theta_c(t) - \hat{\theta}_{c_i}(t) = \text{phase error in the carrier tracking loop of}$$
receiver i.

$n_i'(t)$ = a white Gaussian noise process with one-sided spectral density of N_{oi} watts/Hz.

Let the weighting factor for baseband signal $r_i'(t)$ be α_i. Then the signal combiner output $S(t)$ can be expressed as

$$S(t) = \sum_{i=1}^{n} \alpha_i r_i'(t - \tau_i)$$

$$= \left\{ \sum_{i=1}^{n} \alpha_i \sqrt{P_{D_i}}\, d(t - \tau_i)\, \boxed{5} in\left[\omega_{SC}t + \theta_{SC}(t - \tau_i) - \omega_{SC}\tau_i\right] \right.$$

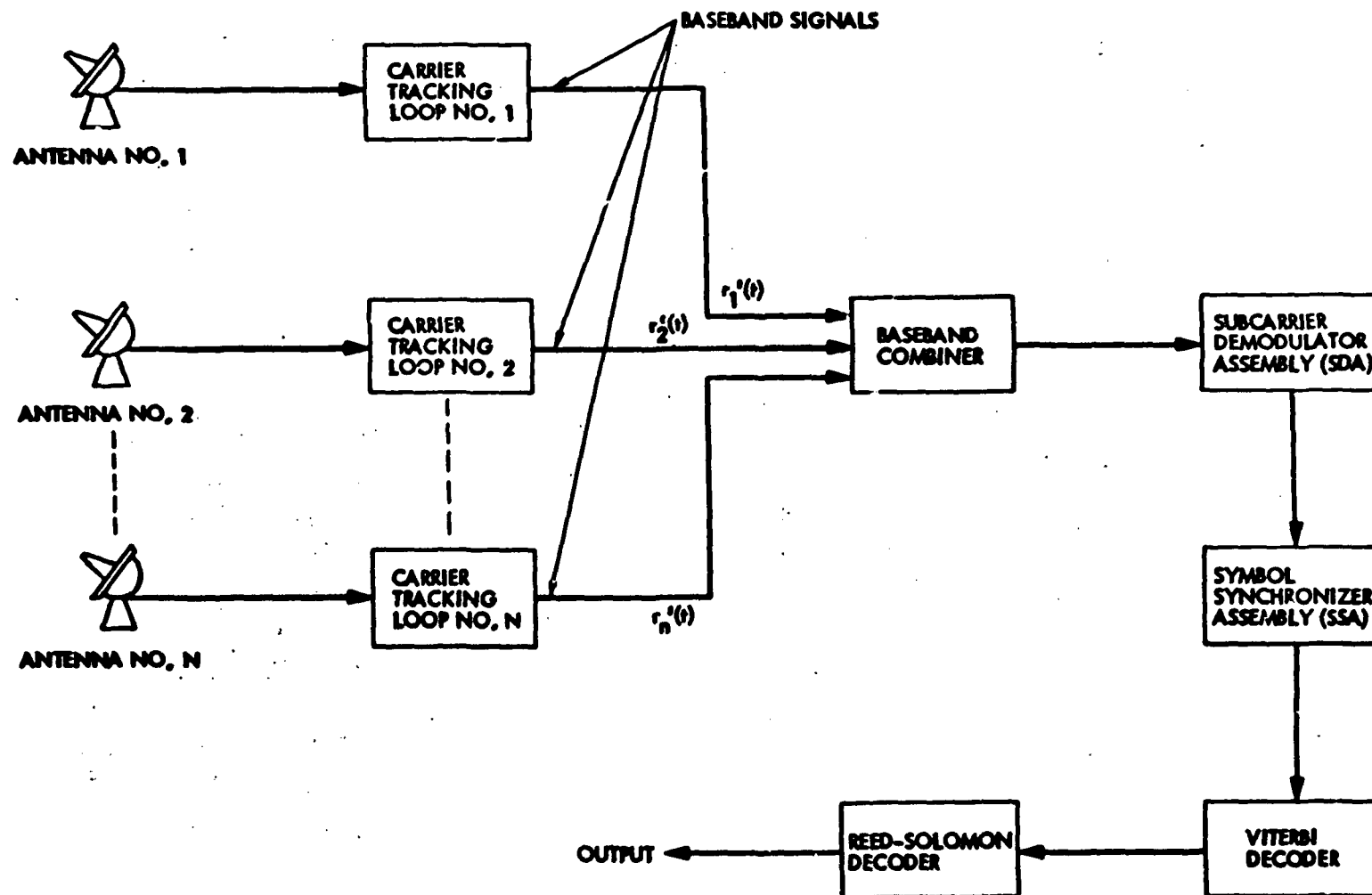$$\left. \times \cos\phi_{c_i}(t - \tau_i) \right\} + n(t) \qquad (27)$$

46

Figure 15. A Simplified Functional Block Diagram of An Antenna Array Combining System

τ_i = delay error in delay tracking loop i relative to the signal from receiver 1, where τ_1 = 0.

$n(t)$ = a white Gaussian noise process with one-sided spectral density of $\sum_{i=1}^{n} \alpha_i^2 N_{oi}$ watts/Hz.

The signal $s(t)$ given in (2) is mixed with the subcarrier signal

$$\mathsf{S} \, in \left[\omega_{SC} t + \hat{\theta}_{SC}(t) \right]$$

in the SDA, where $\hat{\theta}_{SC}(t)$ is the SDA estimated subcarrier phase, and the result is correlated with the estimated BPSK data $d[t - (j - 1) T_s - \epsilon]$ in the SSA, where T_s is the symbol interval and ϵ is the symbol timing error. The result of this correlation is integrated over the symbol time and dumped to the A/D converter at the end of each symbol time to provide an 3-bit soft decision data to the Viterbi decoder. The output of the Viterbi decoder is then fed into the Reed-Solomon decoder. The integrate-and-dump circuit output in the SSA is given by

$$S'(jTs) = \frac{K}{T_s} \int_{(j-1)T_s + \epsilon}^{jT_s + \epsilon} \left\{ \sum_{i=1}^{n} \alpha_i \sqrt{P_{D_i}} \, \mathsf{S} in \left[\omega_{SC} t + \theta_{SC}(t - \tau_i) - \omega_{SC} \tau_i \right] \right.$$

$$\times \mathsf{S} in \left[\omega_{SC} t + \hat{\theta}_{SC}(t) \right] \left[\cos \phi_{c_i}(t - \tau_i) \right] d[t - \tau_i]$$

$$\times \left. d\left[t - (j - 1) Ts - \epsilon \right] \right\} dt + K \, n_1(jTs)$$

Thus

$$S'(jT_s) = \frac{K}{T_s} \int_{(j-1)T_s+\epsilon}^{jT_s+\epsilon} \left\{ \sum_{i=1}^{n} \alpha_i \sqrt{P_{D_i}} \left[1 - \left(\frac{2}{\pi}\right) \left| \phi_{SC}(t, \tau_i) \right| \right] \times \right.$$

$$\left. \left[\cos \phi_{c_i}(t - \tau_i) \right] d\left[t - \tau_i \right] d\left[t - (j-1)T_s - \epsilon \right] dt \right\} + Kn_1(jT_s)$$

where

$$\phi_{SC}(t, \tau_i) = \theta_{SC}[t - \tau_i] - \omega_{SC}\tau_i - \hat{\theta}_{SC}(t)$$

$j = j^{th}$ symbol time.

K = integrate-and-dump circuit gain.

$n_1(jT_s)$ = a zero-mean Gaussian random variable with variance $\sum_{i=1}^{n} \alpha_i^2 N_{oi}/2T_s$ and $n_1(jT_s) \neq n_1(iT_s)$ for $j \neq i$.

If the carrier, subcarrier, combiner delay, and symbol tracking loop bandwidths are much smaller than the symbol rate and if K is set to equal $1/\sqrt{\sum_{i=1}^{n} \alpha_i^2 N_{oi}/2T_s}$, then S'(jTs) becomes

$$S'(jT_s) = \left\{ \sum_{i=1}^{n} \sqrt{E_{b_i} / \sum_{i=1}^{n} \alpha_i^2 N_{oi}} \left[\cos \phi_{c_i}(jT_s - \tau_{ij}) \right] \times \left[1 - \left(\frac{2}{\pi}\right) |\phi_{SC}(jT_s, \tau_{ij})| \right] \right.$$

$$\left. \times \left[1 - 2 |\lambda(jT_s, \tau_{ij})| \right] \right\} + n_2(jT_s) \qquad (28)$$

3-5

49

where

$$\tau_{ij} = \tau_i(jT_s)$$

$$E_{b_i} = P_{D_i} T = \text{energy per bit (Joules/bit)}$$

$$T = \text{bit period}$$

$$\lambda(jT_s, \tau_{ij}) = |\xi(jT_e) - \tau_{ij}|/T_s$$

$$n_2(jT_s) = \text{a zero mean unit variance Gaussian random variable.}$$

From (28), one can see that the signal-to-noise ratio at the matched filter output at the jth symbol time is given by

$$\left\{ \sum_{i=1}^{n} \sqrt{E_{b_i} \Big/ \sum_{i=1}^{n} \alpha_i^2 \, N_{oi}} \left[\cos \phi_{c_i}(jT_s, \tau_{ij}) \right] \times \left[1 - \left(\frac{2}{\pi}\right) \left| \phi_{SC}(jT_s, \tau_{ij}) \right| \right] \times \right.$$

$$\left. \left[1 - 2 \, |\lambda(jT_s, \tau_{ij})| \right] \right\}^2 \tag{29}$$

For perfect delay, subcarrier, and symbol tracking loops, $\tau_{ij} = 0$ for $i=1,---,n$, and $\phi_{SC}(jT_s) = \lambda(jT_s) = 0$. Thus (29) becomes

$$\left[\sum_{i=1}^{n} \sqrt{E_{b_i} \Big/ \sum_{i=1}^{n} \alpha_i^2 \, N_{oi}} \, \cos \phi_{c_i}(jT_s) \right]^2 \tag{30}$$

Now suppose the bit error probability, P_e, of the Viterbi decoder, under perfect carrier tracking loops in the array, is given by

$$P_e = f(E_b/N_o) \tag{31}$$

3-6

where E_b/N_o is the signal-to-noise ratio at the input of the Viterbi decoder. If ϕ_{c_i} for $i=1,2,---,n$ are constant over all Viterbi decoder errors, then by (30) and (31), the conditional bit error probability for constant ϕ_{c_i} $(i=1,...,n)$ is given by

$$P_e\left(\phi_{c_1},\ \phi_{c_2},\ \cdots,\ \phi_{c_n}\right) = f\left\{\left[\sum_{i=1}^{n}\sqrt{E_{b_i}\Bigg/\sum_{i=1}^{n}\alpha_i^2\ N_{oi}}\ \cos\phi_{c_i}\right]^2\right\} \qquad (32)$$

The bit error probability is then given by

$$P_e = \int_{-\pi}^{\pi}--- \int_{-\pi}^{\pi} P_e\left(\phi_{c_1}\ \phi_{c_2},\ \cdots,\ \phi_{c_n}\right)\ P\left(\phi_{c_1},\phi_{c_2},\ \cdots,\ \phi_{c_n}\right)\ d\phi_{c_1}\ d\phi_{c_2}\ --- d\phi_{c_n}$$

$$(33)$$

where $p(\phi_{c_1},\ \phi_{c_2},\ ---,\ \phi_{c_n})$ is the joint probability density of $\phi_{c_1},\ \phi_{c_2},---,\ \phi_{c_n}$. Since $\phi_{c_1},\ \phi_{c_2},\ ---,\ \phi_{c_n}$ are statistically independent, $p(\phi_{c_1},\ \phi_{c_2},\ ---,\ \phi_{c_n})$ in (33) can be expressed as

$$P_e\left(\phi_{c_1},\ \phi_{c_2},\ ---,\ \phi_{c_n}\right) = P\left(\phi_{c_1}\right) P\left(\phi_{c_2}\right) --- P\left(\phi_{c_n}\right) \qquad (34)$$

By (34), (33) becomes

$$P_e = \int_{-\pi}^{\pi}--- \int_{-\pi}^{\pi} P_e\left(\phi_{c_1},\ \phi_{c_2},\ ---,\ \phi_{c_n}\right) P\left(\phi_{c_1}\right) P\left(\phi_{c_2}\right) --- P\left(\phi_{c_n}\right) d\phi_{c_1}\ d\phi_{c_2}\ --- d\phi_{c_n}$$

$$(35)$$

where $p(\phi_{c_i})$ is the probability density of the carrier phase error in receiver i. $p(\phi_{c_i})$ is of the same form as shown in (15) and (17) for one-way and two-way transmission, respectively.

The weighting factor α_i in (32) are selected to maximize the output signal-to-noise ratio of the array combining system. It was shown (Ref. 17) that the output signal-to-noise ratio of the array combining system given by

$$\frac{E_b}{N_0} = \frac{\left(\sum_{i=1}^{n} \alpha_i \sqrt{P_{D_i}}\right)^2 T}{\sum_{i=1}^{n} \alpha_i^2 N_{oi}}$$

is maximized when

$$\alpha_1 = 1$$

and

$$\alpha_i = \frac{\sqrt{P_{D_i}}/N_{oi}}{\sqrt{P_{D_1}}/N_{o1}} , \quad \text{for} \quad i=2,3,\ldots,n$$

Under these conditions, E_b/N_o becomes

$$\frac{E_b}{N_o} = \sum_{i=1}^{n} \frac{E_{b_i}}{N_{oi}} = \frac{E_{b_1}}{N_{o1}} G \tag{36}$$

where

$$G = 1 + \sum_{i=1}^{n} \frac{E_{b_i}/N_{oi}}{E_{b_1}/N_{o1}}$$

is the improved signal-to-noise ratio.

By (32), P_e in (35) can be expressed as a function of E_b/N_o as

follows:

$$P_e = \int_{-\pi}^{\pi} --- \int_{-\pi}^{\pi} f\left[\frac{E_b}{N_o}\left(\sum_{i=1}^{n} \beta_i \cos \phi_{c_i}\right)^2\right] \times$$

$$\left[\prod_{i=1}^{n} p\left(\phi_{c_i}\right)\right] d\phi_{c_1} d\phi_{c_2} --- d\phi_{c_n} \tag{37}$$

where

$$\beta_i = \sqrt{E_{b_i} \bigg/ \sum_{i=1}^{n} \alpha_i^2 N_{oi}} \bigg/ \sqrt{E_b/N_o}$$

If identical antennas and receivers are used in the array, then $\alpha = \alpha_i = 1$, $E_{b_i}/N_{oi} = \frac{1}{n}(E_b/N_o)$, and $\beta_i = 1/n$ for $i=1,2,\ldots,n$. In this case (37) becomes

$$P_e = \int_{-\pi}^{\pi} --- \int_{-\pi}^{\pi} f\left\{\frac{E_b}{N_o}\frac{1}{n^2}\left[\sum_{i=1}^{n} \cos\phi_{c_i}\right]^2\right\} \times \left[\prod_{i=1}^{n} p(\phi_{c_i})\right] d\phi_{c_1} d\phi_{c_2} --- d\phi_{c_n}$$

$$\tag{38}$$

Since a Costas loop has a 15 to 30 dB tracking loop SNR advantage over a phase-locked loop, it may be beneficial in some cases to use Costas loop receivers to minimize the effects of receiver phase errors. In an array combining system with Costas loop receivers, the combining is done at the IF level. The output of the combiner $S(t)$ can be expressed as

53

$$S(t) = \left\{ \sum_{i=1}^{n} \alpha_i \sqrt{2P_{D_i}}\; d(t - \tau_i)\; \cos\left[\omega_{IF}t + \hat{\theta}_{c_i}(t - \tau_i) - \omega_{IF}\tau_i\right] \right\} + n(t)$$

(39)

where

$$\hat{\theta}_{c_i}(t) = \text{the Costas loop estimated carrier phase in receiver i.}$$

The signal is mixed with $\sqrt{2}\cos\left[\omega_{IF}t + \theta_c(t)\right]$ to give

$$S'(t) = \left\{ \sum_{i=1}^{n} \alpha_i \sqrt{P_{D_i}}\; d(t - \tau_i)\; \cos\left[\omega_{IF}t + \phi_{c_i}(t, \tau_i)\right] \right\} + n(t)$$

(40)

where

$$\phi_{c_i}(t, \tau_i) = \hat{\theta}_{c_i}(t - \tau_i) - \omega_{IF}\tau_i - \theta_c(t).$$

A comparison between (27) and (40) shows that if $\tau_i = 0$ for $i=1,2,\ldots,n$, then these two equations are identical except for the subcarrier term. Thus, assuming a perfect symbol synchronizer, one will get an equation similar to the one given in (37), i.e.,

$$Pe = \int_{-\pi/2}^{\pi/2} \cdots \int_{-\pi/2}^{\pi/2} f\left\{ \frac{E_b}{N_o}\left(\sum_{i=1}^{n}\beta_i \cos\phi_{c_i}\right)^2 \right\} \times \prod_{i=1}^{n} p(\phi_{c_i})\; d\phi_{c_1} d\phi_{c_2} \cdots d\phi_{c_n}$$

(41)

If identical antenna and receivers are used, then $\alpha_i = \alpha_1$, $\rho_i = \rho$, $E_{b_i} = E_b$, and $N_{oi} = N_o$, and $\beta_i = 1/n$. Thus (43) becomes

$$Pe = \int_{-\pi/2}^{\pi/2} \cdots \int_{-\pi/2}^{\pi/2} f\left\{\frac{E_b}{N_o} \frac{1}{n^2}\left[\sum_{i=1}^{n} \cos\phi_{c_i}\right]^2\right\} \times \prod_{i=1}^{n} p(\phi_{c_i}) \, d\phi_{c_1} \, d\phi_{c_2} \cdots d\phi_{c_n}$$

(42)

Thus by (37) and (41), one can express the bit error probability, P_e, on the Viterbi decoder output as a function of the signal-to-noise ratio of the array combining system for baseband and IF combining, respectively.

Let the symbol error probability of the Viterbi decoder for an ideal receiver be given by $g(E_b/N_o)$. Then the symbol error probability for constant carrier phase errors ϕ_{c_i}, where $i=1,2,\ldots,n$, is given by

$$g\left[\frac{E_b}{N_o}\left(\sum_{i=1}^{n} \beta_i \cos\phi_{c_i}\right)^2\right]$$

Thus by the same procedure discussed in Section II, one can obtain the theoretical performance of the concatenated RS/Viterbi coding system for array combining. The bit error rate versus E_b/N_o curves for the Viterbi channel and the RS/Viterbi channel in a one-way communication with identical antennas and receivers in the array combining system are shown in Figs. 16 and 17 for carrier tracking loop SNR of 11 and 12 dB, respectively.

3-11

From these curves one can see the following facts:

(1)   A coded array combining system is less sensitive to downlink
carrier phase tracking error than a coded single antenna system.

(2)   In an array combining system the concatenated RS/Viterbi coded
channel still has significant coding gains over a Viterbi-decoded
channel at very low error probability ($\leq 10^{-6}$) for a weak
downlink.

The same conclusions can also be made for the case of two-way communication with
a weak uplink and weak downlink. Thus based on both the analytical and the test
results given in Sections II and III for the single antenna and the array combin-
ing system, respectively, one can see that the concatenated RS/Viterbi channel
is a very effective scheme for providing reliable communication under weak link
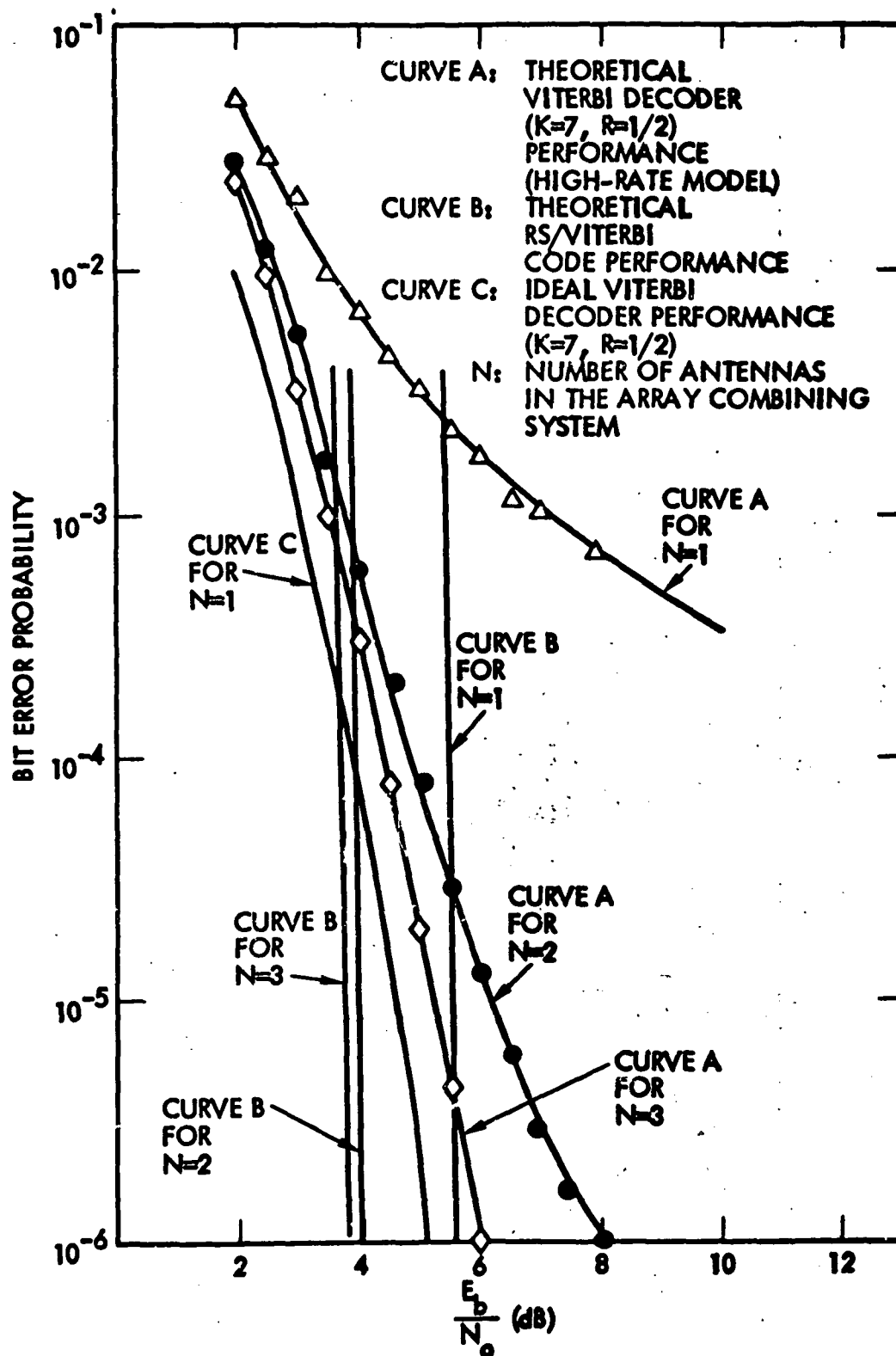conditions.

56

Figure 16. Coded Array Combining System Performance (Carrier Loop SNR = 11 dB)
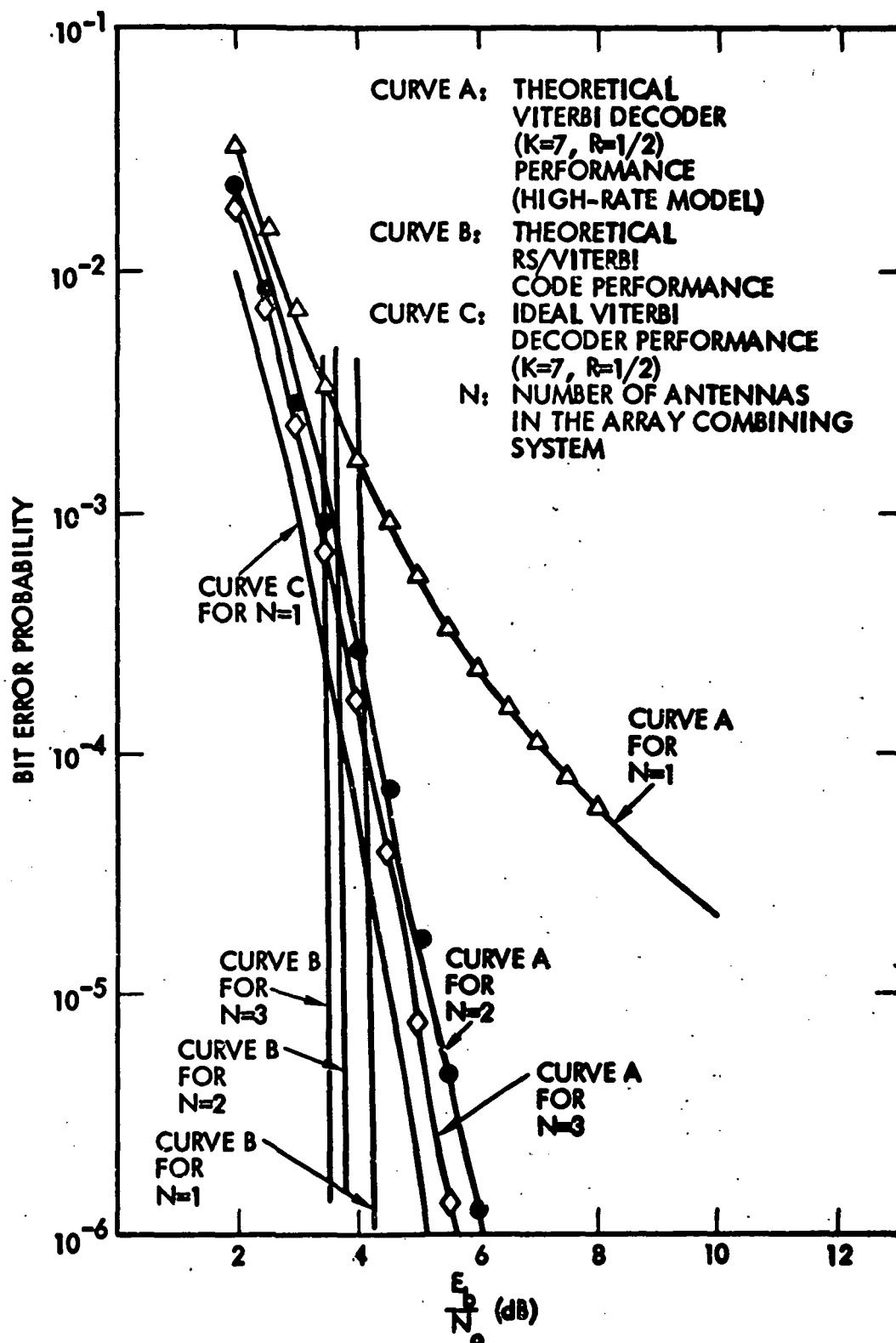
3-13

57

Figure 17. Coded Array Combining System Performance (Carrier Loop SNR = 12 dB)

58

IV. CONCLUSIONS

Both analytical and experimental measurements of the effects of receiver tracking phase error on the performance of the concatenated RS/Viterbi channel coding system have been presented in this document. These measurements were obtained under an emulated S-Band uplink and X-Band downlink, two-way space communication channel. It is shown that the RS/Viterbi coding scheme has large coding gains over the Viterbi-decoded convolutional-only coding system when operated in a weak uplink or a weak downlink, or both, RF environment. It is also shown that if the Viterbi decoder maintains its node synchronization, then performance equivalent to ideal interleaving is obtained with an interleaving depth greater than or equal to 4.

It is further shown that because of the large coding gains of the RS/Viterbi coding scheme, using this coding system will permit the transmission of high-rate data in conjunction with two-way ranging or doppler measurements when operated in the weak uplink and weak downlink conditions in a two-way space communication. The RS/Viterbi coding scheme also offers more data rate protection than the Viterbi-decoded convolutional-only coding system in one-way communication.

Finally, the effect of receiver phase errors on the performance of the concatenated RS/Viterbi coding system with array combining is discussed. It is shown that in an array combining system the concatenated RS/Viterbi coded channel still has significant coding gains over a Viterbi-decoded channel. Thus the concatenated RS/Viterbi coded channel is a very effective scheme for providing reliable communication under weak link conditions.

REFERENCES

[1] Forney, G. D., Concatenated Codes, the MIT Press, Cambridge, MASS., 1966.

[2] Odenwalder, J. P., "Optimum Decoding of Convolutional Codes," Ph.D. dissertation, Syst. Sci. Dept., Univ. of California, Los Angeles, 1970.

[3] Odenwalder, J. P., et al, "Hybrid Coding System Study," submitted to NASA Ames Research Center by Linkabit Co., San Diego, California, Final Report, Contract No. NAS-2-6722, Sept. 1972.

[4] Rice, R. F., "Channel Coding and Data Compression System Considerations for Efficient Communication of Planetary Imaging Data," Technical Memorandum 33-695, Jet Propulsion Laboratory, Pasadena, CA., June 1974.

[5] Rice, R. F., "An Advanced Imaging Communication System for Planetary Exploration," Proceedings of 1975 SPIE Conference, Vol. 66, San Diego, CA., Aug. 1975.

[6] Rice, R. F., "Potential End-to-End Imaging Information Rate Advantages of Various Alternative Communication Systems," JPL Publication 78-52, June 15, 1978.

[7] Odenwalder, J. P., "Concatenated Reed-Solomon/Viterbi Channel Coding for Advanced Planetary Missions: Analysis, Simulations, and Tests," submitted to Jet Propulsion Laboratory by Linkabit Co., San Diego, CA, Contract No. 953866, Dec. 1974.

[8] Rice, R. F. et al, "Block Adaptive Rate Controlled Image Data Compression," Proceedings of 1979 National Telecommunication Conference, Washington, D.C., Nov. 1979.

[9] Rice, R. F., "Some Practical Universal Noiseless Coding Techniques," Proceedings of 1979 SPIE Conference, San Diego, CA., Aug. 1979.

[10] Liu, K. Y., and Lee, J. J., "An Experimental Study of the Concatenated Reed-Solomon/Viterbi Channel Coding System Performance and Its Impact on Space Communication," JPL Publication 81-58.

[11] Deep Space Network Functional Requirements, Large Advanced Antenna Station, Nov. 1978, JPL Internal Document 820-30.

[12] Viterbi, A. J., "Principle of Coherent Communication", McGraw-Hill Book Co., 1966.

[13] Tausworthe, R. C., "Theory and Practical Design of Phase-Locked Receivers", Vol. 1, JPL TR. No. 32-819.

[14] Simon, M. K., "On the Selection of an Optimum Design Point for Phase Coherent Receivers Employing Bandpass Limiters", IEEE Trans. Comm., April 1972, pp. 210-214.

[15] Lindsey, W. C., and Simon, M. K., Telecommunication System Engineering, Prentice-Hall, Inc., 1973.

[16] Wilck, H., "A Signal Combiner for Antenna Arraying," JPL DSN Progress Report 42-25, pp. 111-117.

[17] Winkelstein, R. A., "Analysis of the Signal Combiner for Multiple Antenna Arraying," JPL DSN Progress Report 42-26, pp. 102-118.

[18] DSN/Flight Project Interface Design, JPL Internal Document 810-5, Rev. D.